

month	NO (ppb)	NO ₂ (ppb)	T (°C)	RH (%)
Härkingen				
4	14.7 (<LOD – 218.3)	17.0 (1.1 – 75.9)	9.5 (-2.3 – 24.5)	64.0 (18.8 – 96.6)
5	13.8 (<LOD – 190.6)	16.4 (0.9 – 60.4)	15.2 (2.3 – 32.1)	67.7 (24.8 – 94.7)
6	13.0 (<LOD – 143.6)	17.0 (1.0 – 57.5)	20.6 (6.4 – 33.9)	64.0 (22.0 – 90.9)
7	15.1 (<LOD – 128.1)	15.5 (1.1 – 55.9)	18.6 (11.8 – 30.6)	70.4 (37.2 – 91.0)
Zurich				
8	2.5 (<LOD – 53.7)	11.6 (0.0 – 43.6)	21.5 (12.2 – 33)	66.9 (28.9 – 92.6)
9	4.7 (<LOD – 102.9)	12.7 (1.4 – 51.1)	14.8 (7.0 – 25.8)	70.9 (37.2 – 94.0)
10	11.8 (<LOD – 164.3)	17 (1.6 – 52.2)	12.7 (2.5 – 23.3)	72.7 (24.9 – 98)
11	11 (<LOD – 135.7)	16.6 (2.1 – 46.3)	6.4 (0.4 – 17.2)	75.2 (36 – 92.9)
Lausanne				
8	10.4 (<LOD – 109.2)	19.1 (1.1 – 69.7)	21.8 (12.6 – 34.9)	60.3 (27.7 – 90.5)
9	14.0 (<LOD – 266.5)	19.4 (1.2 – 71.2)	15.2 (8.7 – 25.8)	65.9 (31.5 – 87.8)
10	17.5 (0.2 – 178.8)	21.1 (1.1 – 64.6)	13.2 (3.8 – 21.1)	66.2 (34.4 – 89)
11	18.2 (0.4 – 201.1)	19.5 (1.2 – 67.7)	6.4 (0.5 – 15.2)	70.7 (38.6 – 90.3)

Table S1: Monthly summary statistics for the calibration and deployment sites. Mean and range (within brackets) are shown for all investigated months. LOD for NO reference instruments is ca. 0.2 ppb

NO

	MAE (ppb)			MBE (ppb)			R ² –			RMSE (ppb)		
	Minimal	Basic	S. Red.	Minimal	Basic	S. Red.	Minimal	Basic	S. Red.	Minimal	Basic	S. Red.
	F. Red.	F. Red.	F. Red.	F. Red.	F. Red.	F. Red.	F. Red.	F. Red.	F. Red.	F. Red.	F. Red.	F. Red.
MLR	4.6 ± 1.0	4.3 ± 0.9	4.4 ± 1.1	4.6 ± 0.9	-0.5 ± 1.5	-0.1 ± 0.8	-1.1 ± 1.4	-1.3 ± 1.3	0.84 ± 0.06	0.86 ± 0.05	0.84 ± 0.07	0.85 ± 0.05
SVR	3.7 ± 1.0	3.1 ± 0.8	3.8 ± 1.2	3.4 ± 0.9	-0.4 ± 1.9	0.1 ± 1.2	-0.3 ± 2.1	0.5 ± 1.4	0.88 ± 0.07	0.91 ± 0.05	0.87 ± 0.07	0.90 ± 0.05
RF	3.7 ± 1.1	3.0 ± 1.0	3.8 ± 1.2	3.0 ± 1.0	-0.5 ± 1.8	-0.4 ± 1.0	-0.6 ± 1.9	-0.4 ± 1.0	0.87 ± 0.06	0.91 ± 0.05	0.87 ± 0.07	0.90 ± 0.05

NO₂

	MAE (ppb)			MBE (ppb)			R ² –			RMSE (ppb)		
	Minimal	Basic	S. Red.	Minimal	Basic	S. Red.	Minimal	Basic	S. Red.	Minimal	Basic	S. Red.
	F. Red.	F. Red.	F. Red.	F. Red.	F. Red.	F. Red.	F. Red.	F. Red.	F. Red.	F. Red.	F. Red.	F. Red.
MLR	4.6 ± 1.3	4.4 ± 1.1	4.3 ± 1.1	4.3 ± 0.4	-0.2 ± 0.5	-1.1 ± 0.2	0.6 ± 0.6	-0.8 ± 0.2	0.66 ± 0.17	0.69 ± 0.16	0.70 ± 0.12	0.71 ± 0.08
SVR	4.1 ± 0.9	3.4 ± 0.6	4.2 ± 0.5	3.2 ± 0.6	-1.0 ± 1.2	-0.6 ± 1.0	0.0 ± 0.8	-0.6 ± 0.7	0.72 ± 0.10	0.79 ± 0.06	0.71 ± 0.06	0.82 ± 0.06
RF	4.4 ± 0.9	3.3 ± 0.9	4.1 ± 0.5	3.1 ± 0.7	-0.1 ± 1.0	-0.7 ± 0.8	0.3 ± 0.9	-0.5 ± 0.6	0.69 ± 0.11	0.81 ± 0.09	0.73 ± 0.04	0.84 ± 0.05

Table S2: Comparison of algorithms' performance using the 4 main models in Appendix A in the main manuscript. Mean value ± standard deviation for each index are shown. MAE stands for Mean Absolute Error, MBE for Mean Bias Error, R² for the coefficient of determination and RMSE for the root mean of square errors.

Algorithm	MAE (ppb)	MBE (ppb)	R ² –	RMSE (ppb)
NO				
RF	3.0 ± 0.9	-0.3 ± 1.1	0.91 ± 0.04	5.0 ± 2.0
NO ₂				
RF	2.7 ± 0.8	-0.2 ± 0.5	0.89 ± 0.03	3.4 ± 1.1

Table S3: Performance of a RF model using both SUs for each site, i.e. 8 EC sensors (see the main manuscript). Mean value ± standard deviation for each index are shown. MAE stands for Mean Absolute Error, MBE for Mean Bias Error, R² for the coefficient of determination and RMSE for the root mean of square errors.

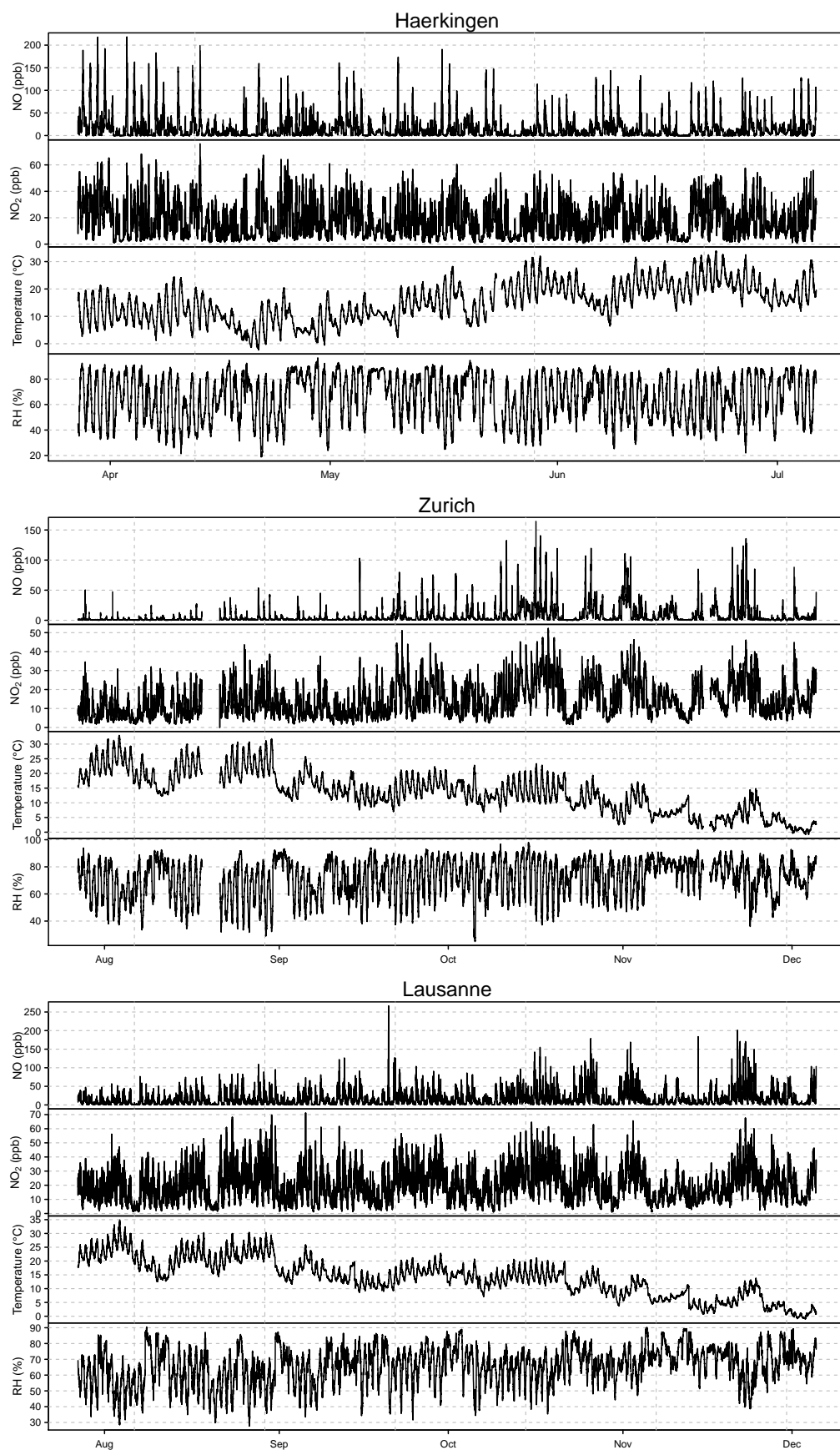


Figure S1: Time series of data collected at the Häerkingen, Zurich and Lausanne reference sites.

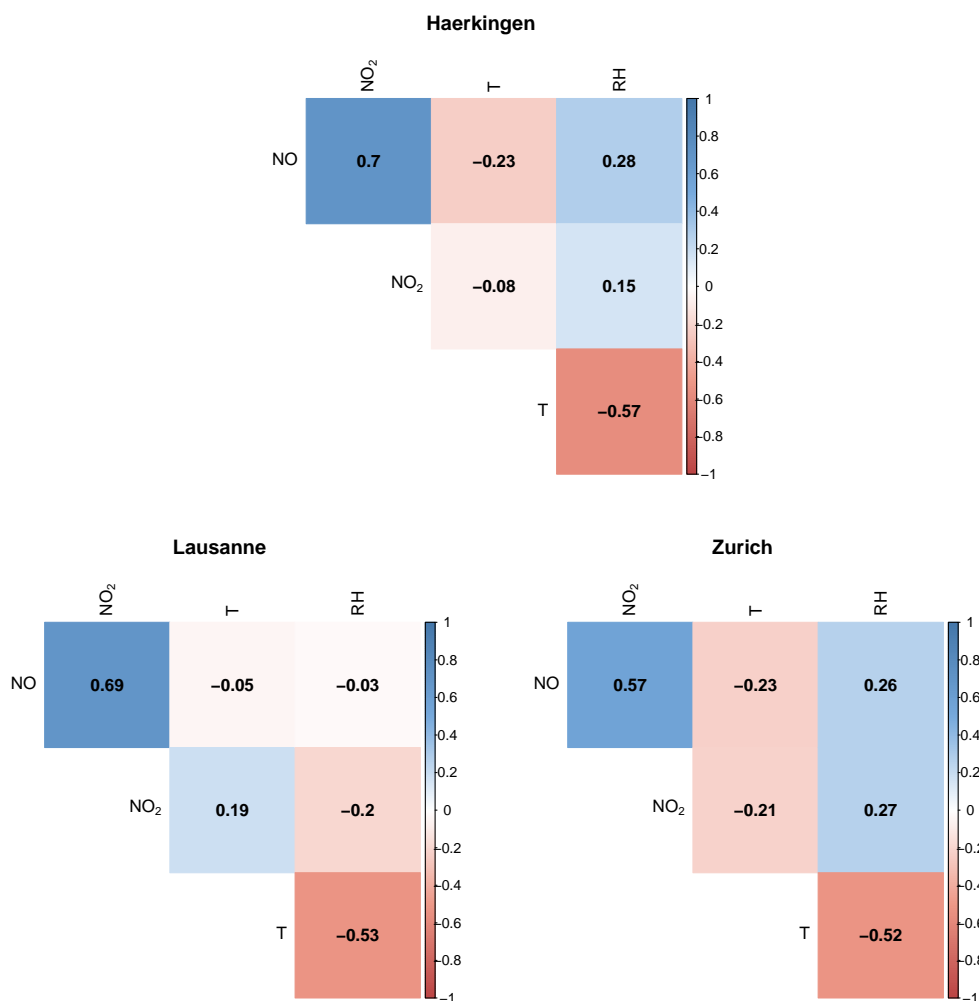


Figure S2: Correlation matrix for meteorological variables and pollutant concentration at the calibration and deployment sites.

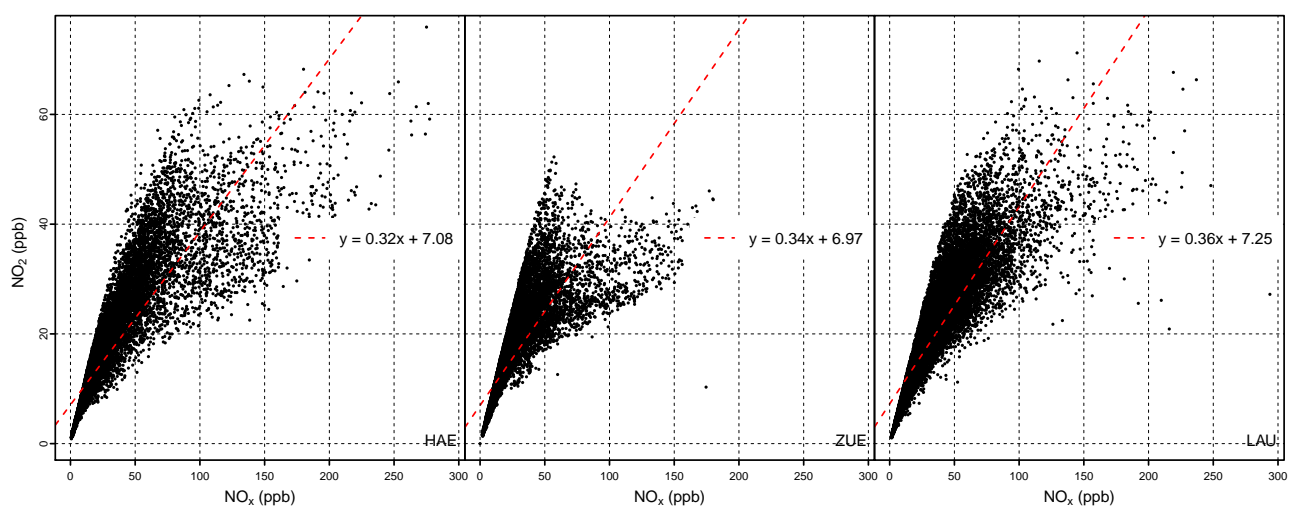


Figure S3: Scatterplot of NO₂ and NO_x at the three sites. Red dashed line indicates the linear regression model.

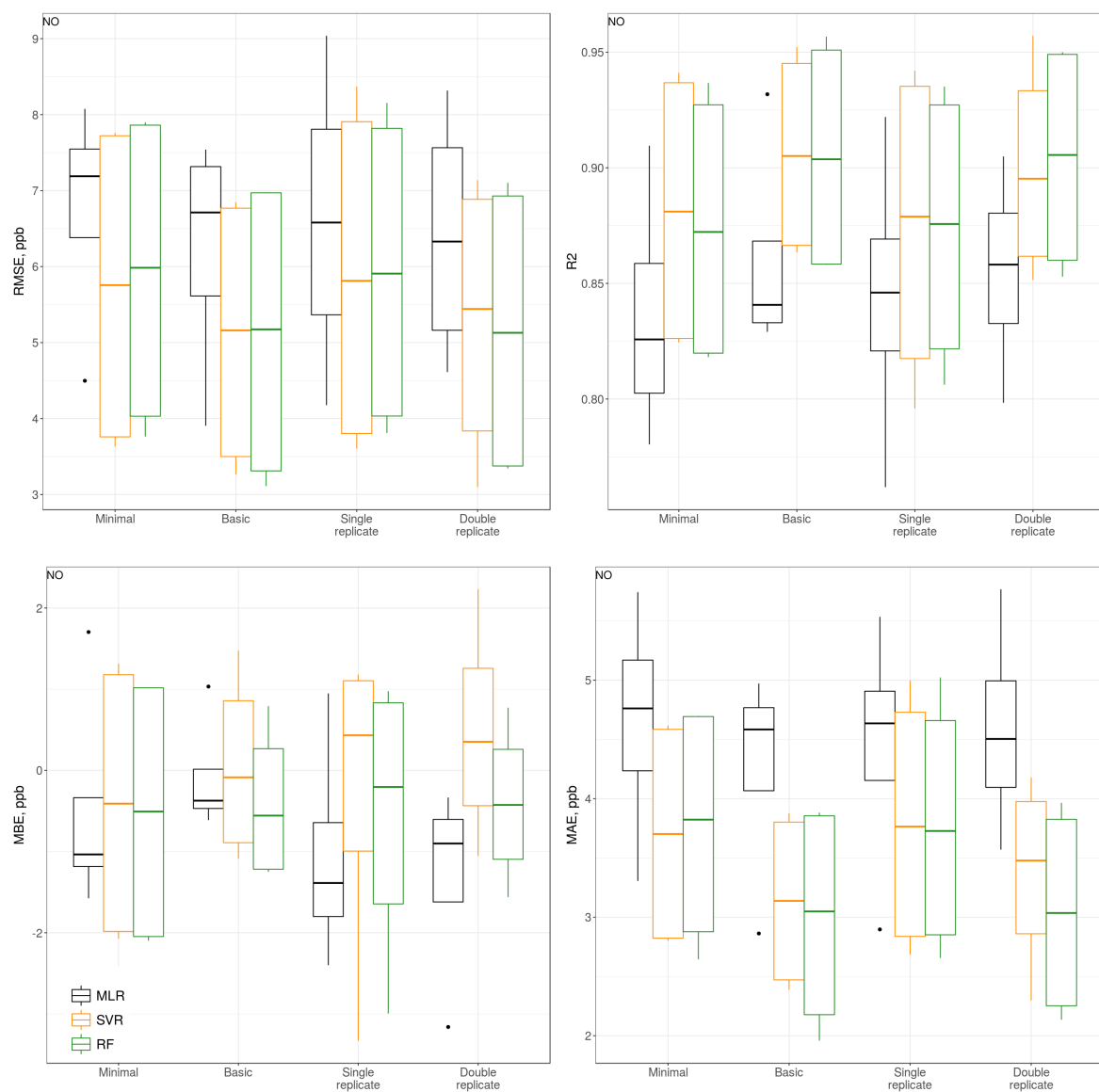


Figure S4: Comparison of goodness-of-fit indexes for the 4 main models listed in Appendix A for the prediction of NO.

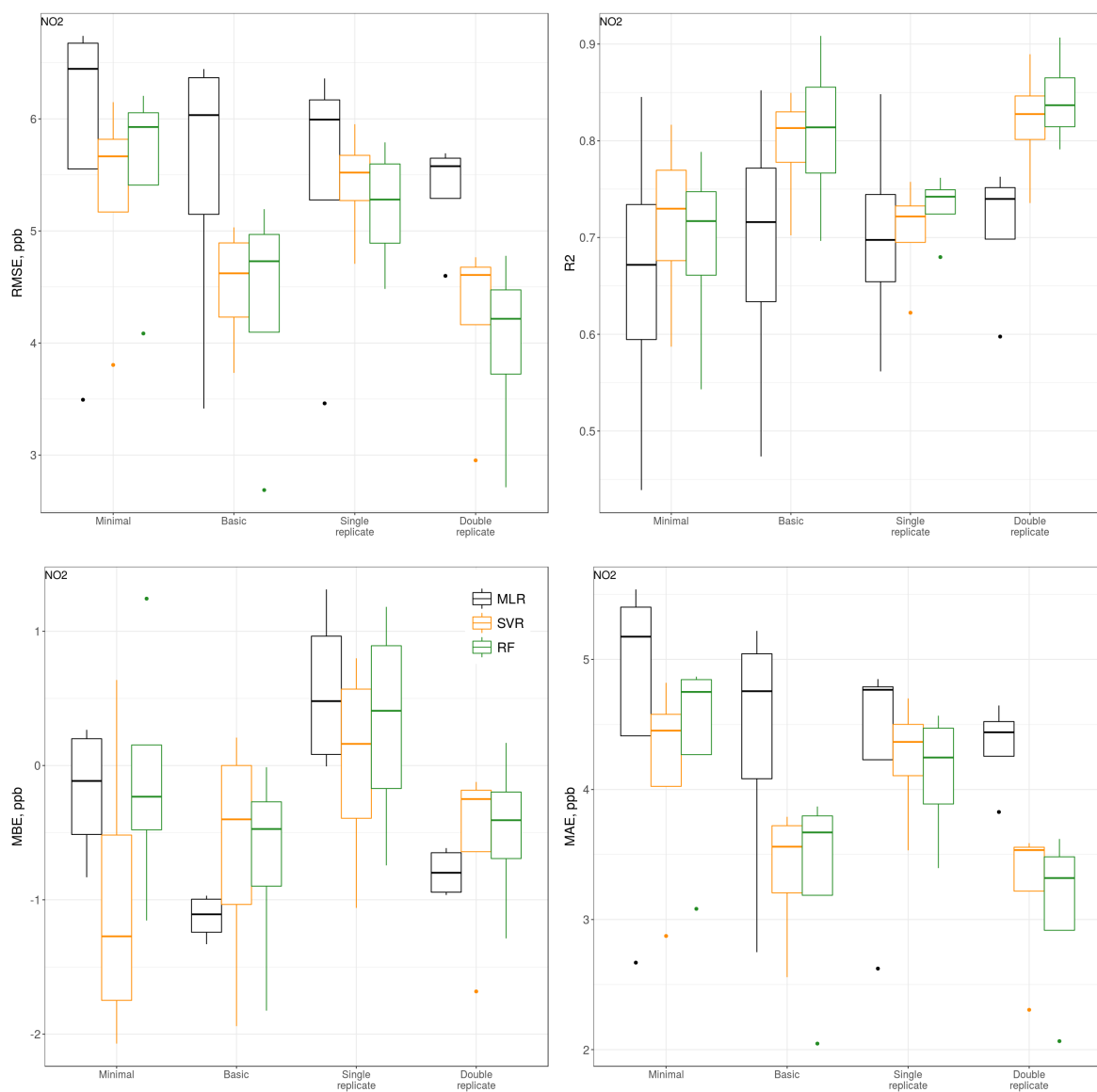


Figure S5: Comparison of goodness-of-fit indexes for the 4 main models listed in Appendix A for the prediction of NO₂.

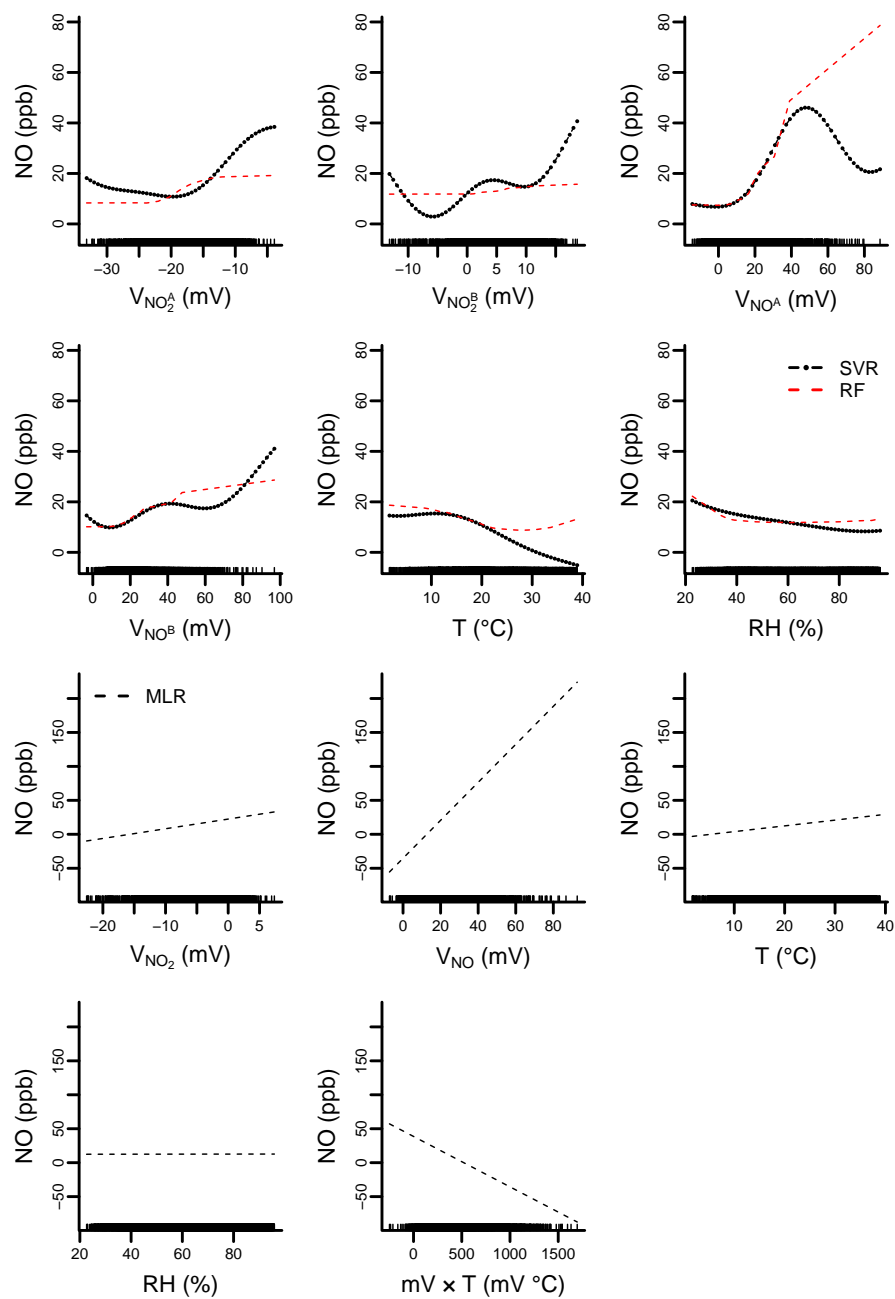


Figure S6: Partial plots for SVM, RF and MLR for the calibration dataset from SU010, NO. Rug on the abscissa indicates the range of the covariate.

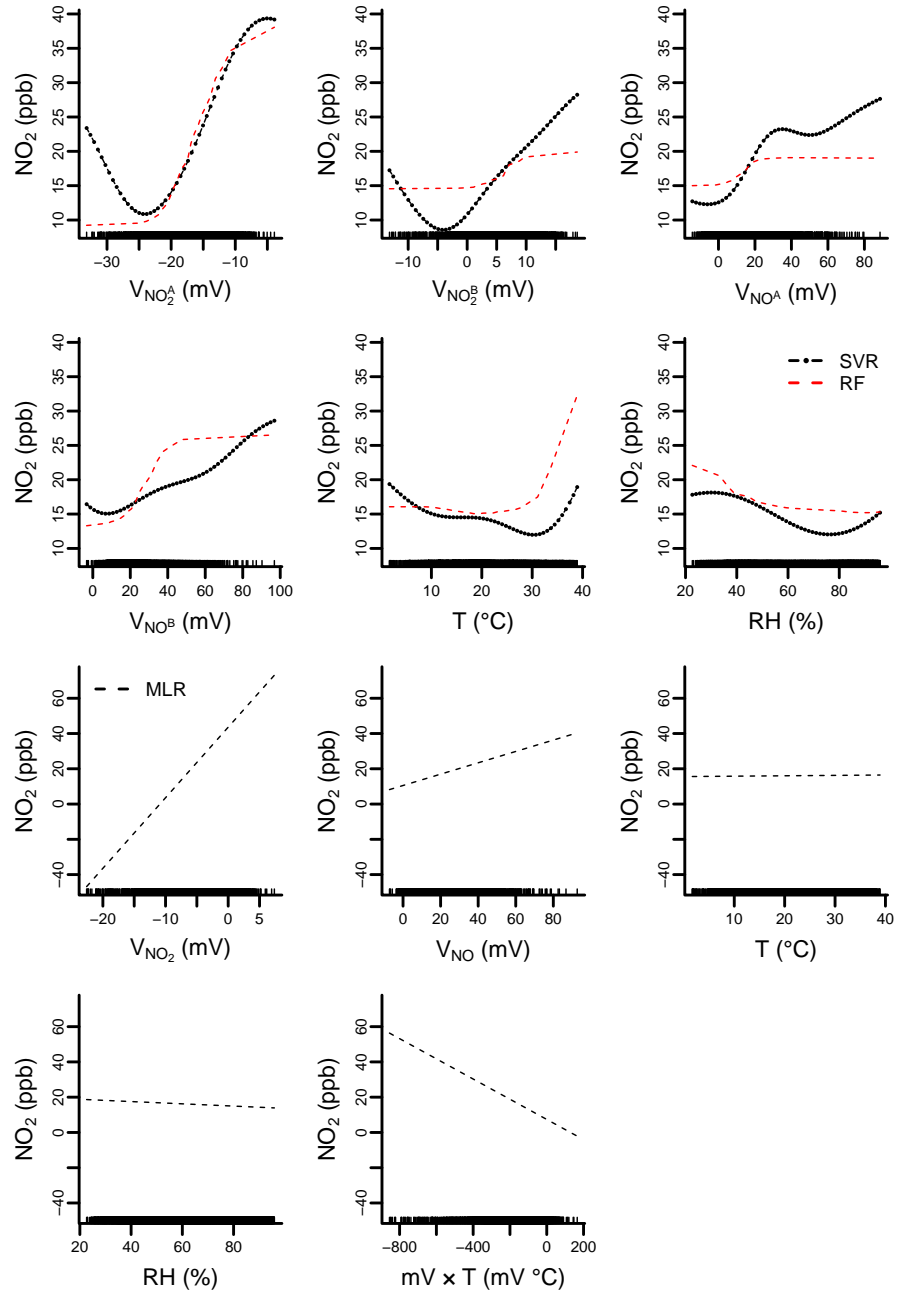


Figure S7: Partial plots for SVM, RF and MLR for the calibration dataset from SU010, NO_2 . Rug on the abscissa indicates the range of the covariate.

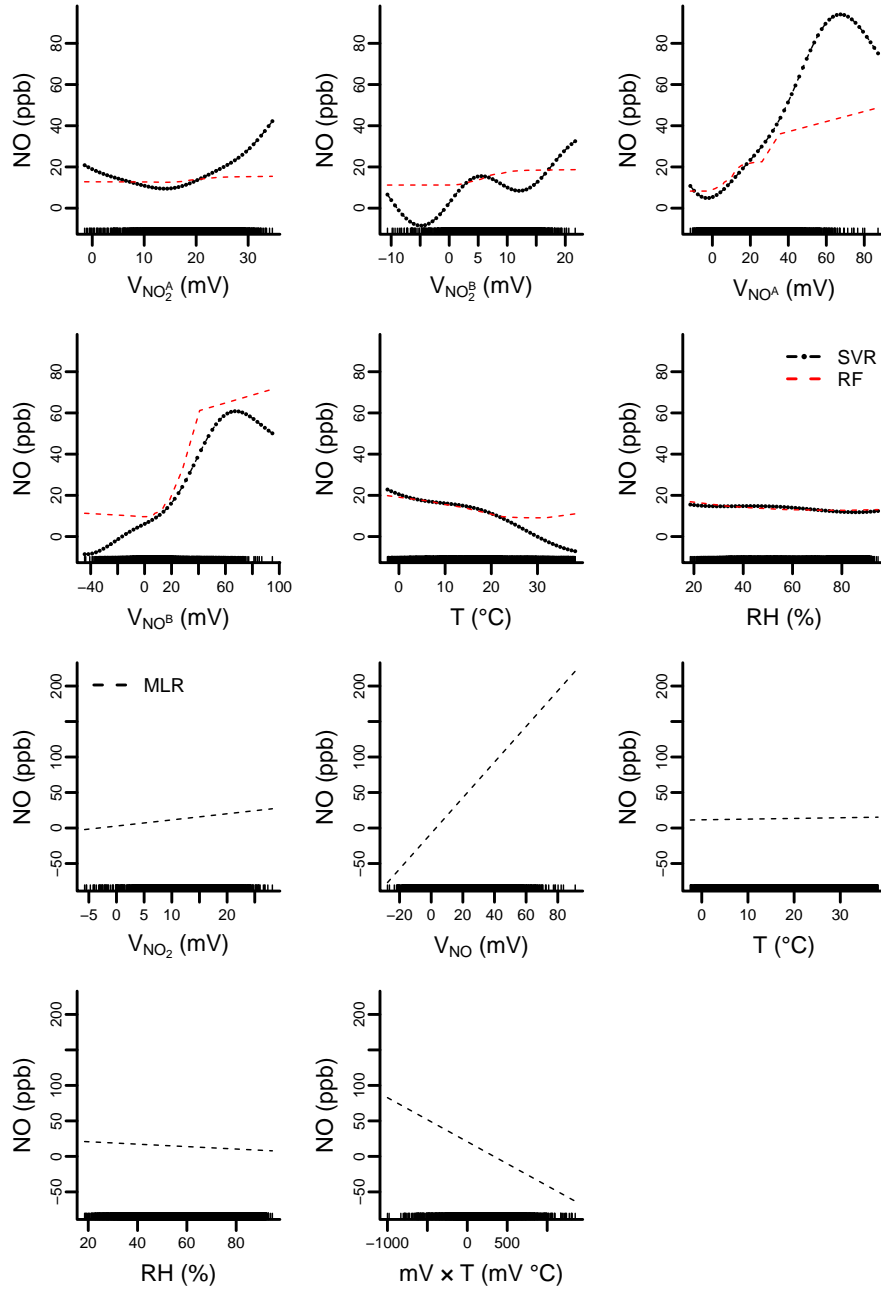


Figure S8: Partial plots for SVM, RF and MLR for the calibration dataset from SU011, NO. Rug on the abscissa indicates the range of the covariate.

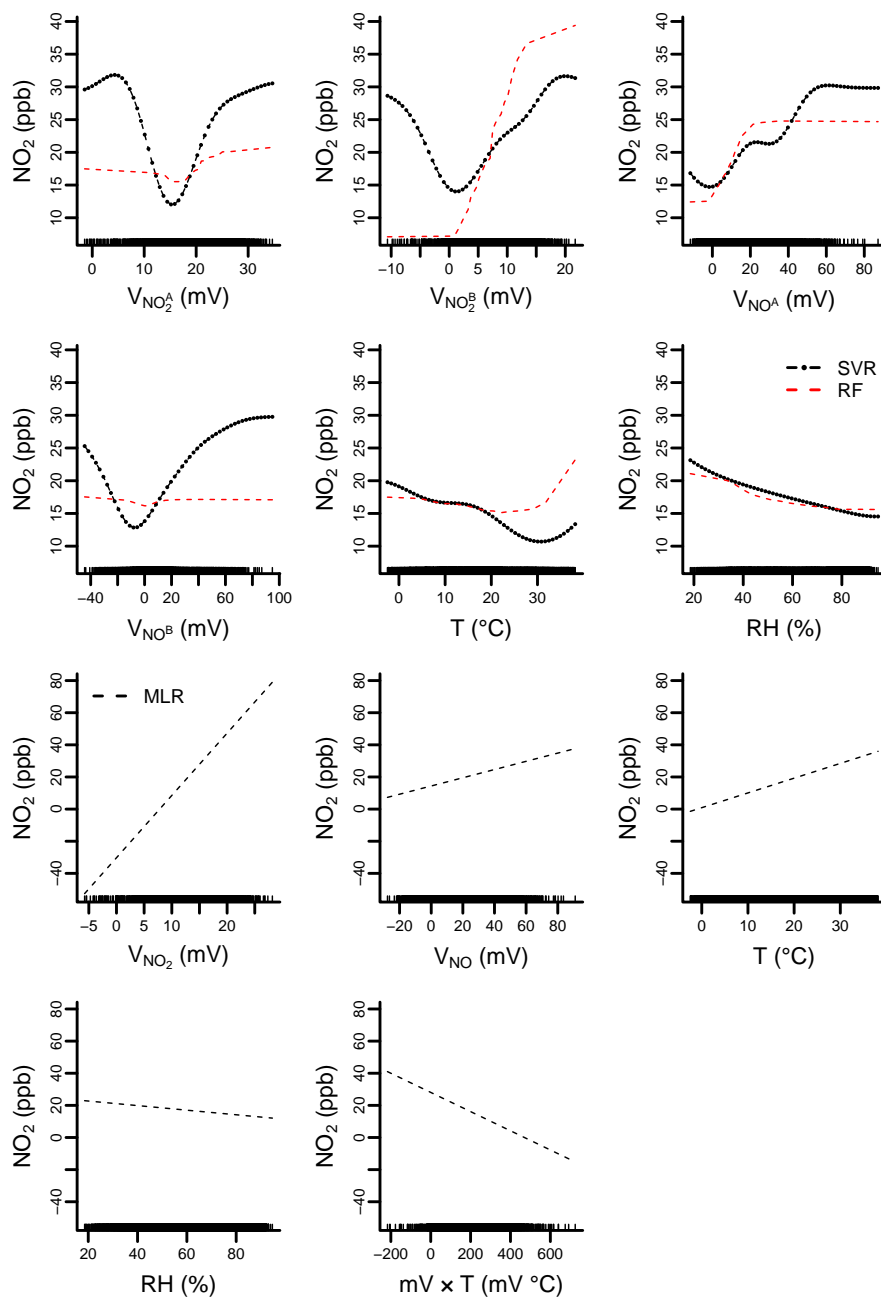


Figure S9: Partial plots for SVM, RF and MLR for the calibration dataset from SU011, NO_2 . Rug on the abscissa indicates the range of the covariate.

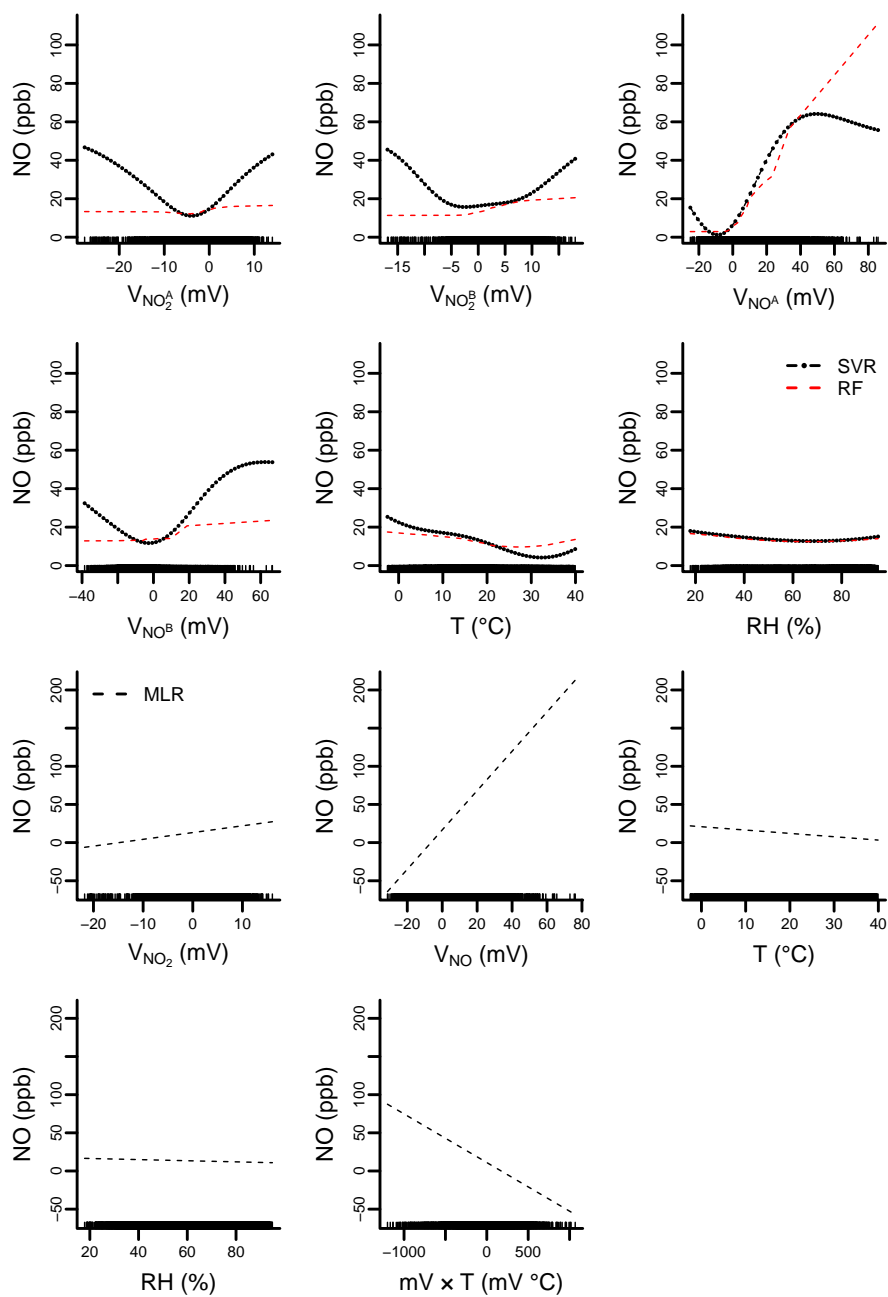


Figure S10: Partial plots for SVM, RF and MLR for the calibration dataset from SU012, NO. Rug on the abscissa indicates the range of the covariate.

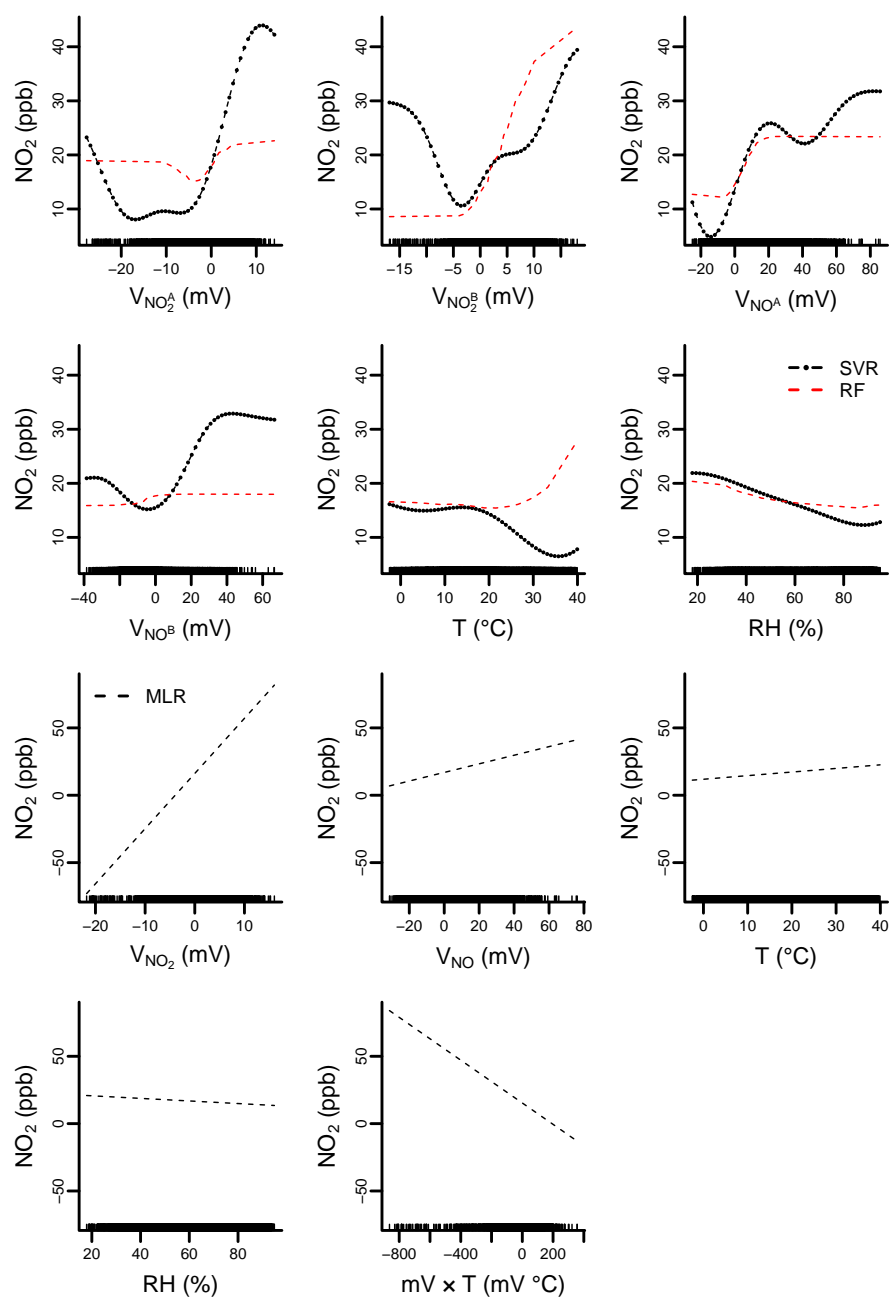


Figure S11: Partial plots for SVM, RF and MLR for the calibration dataset from SU012, NO_2 . Rug on the abscissa indicates the range of the covariate.

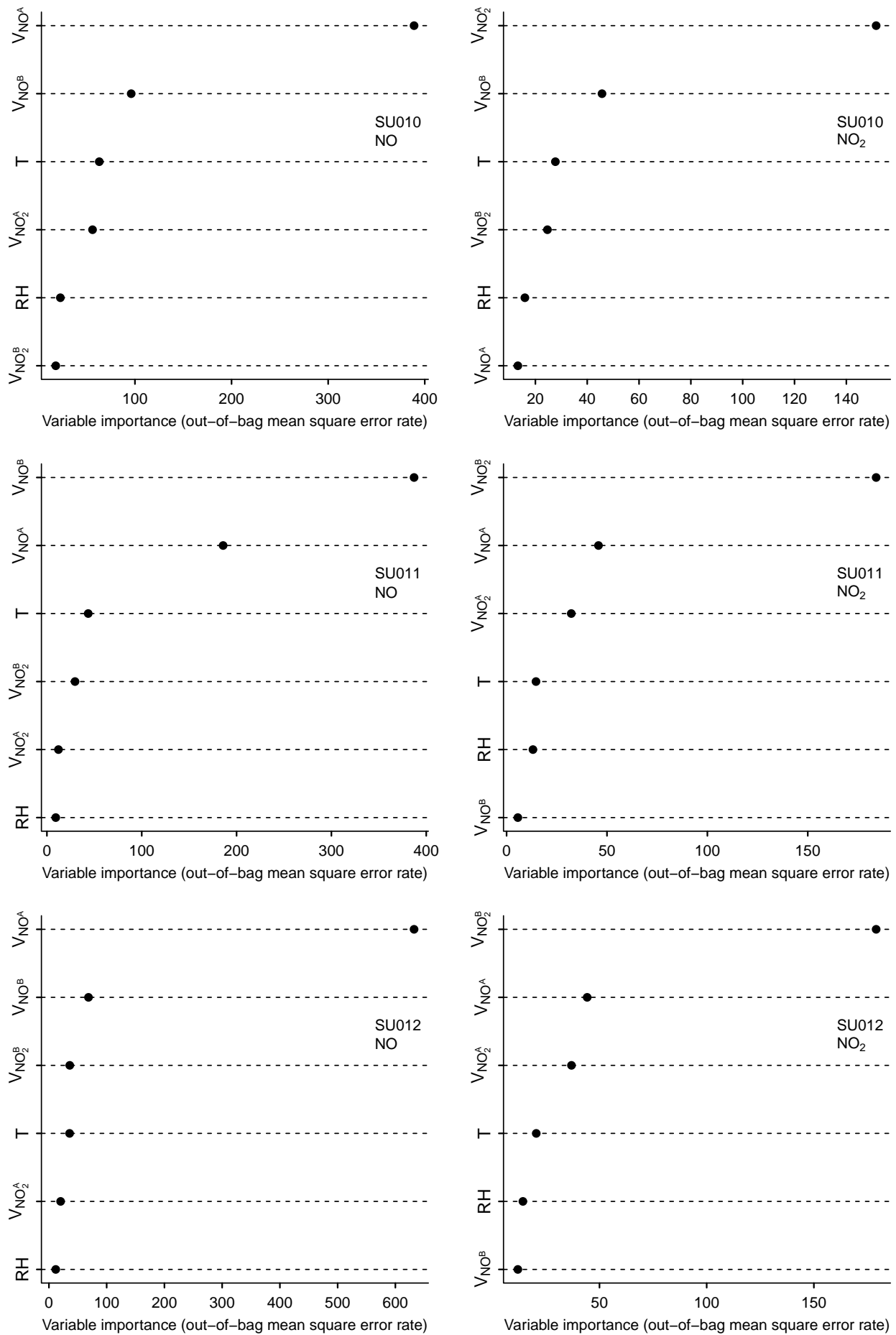


Figure S12: Variable importance plot for the prediction by SU010, SU011 and SU012 of NO and NO₂.

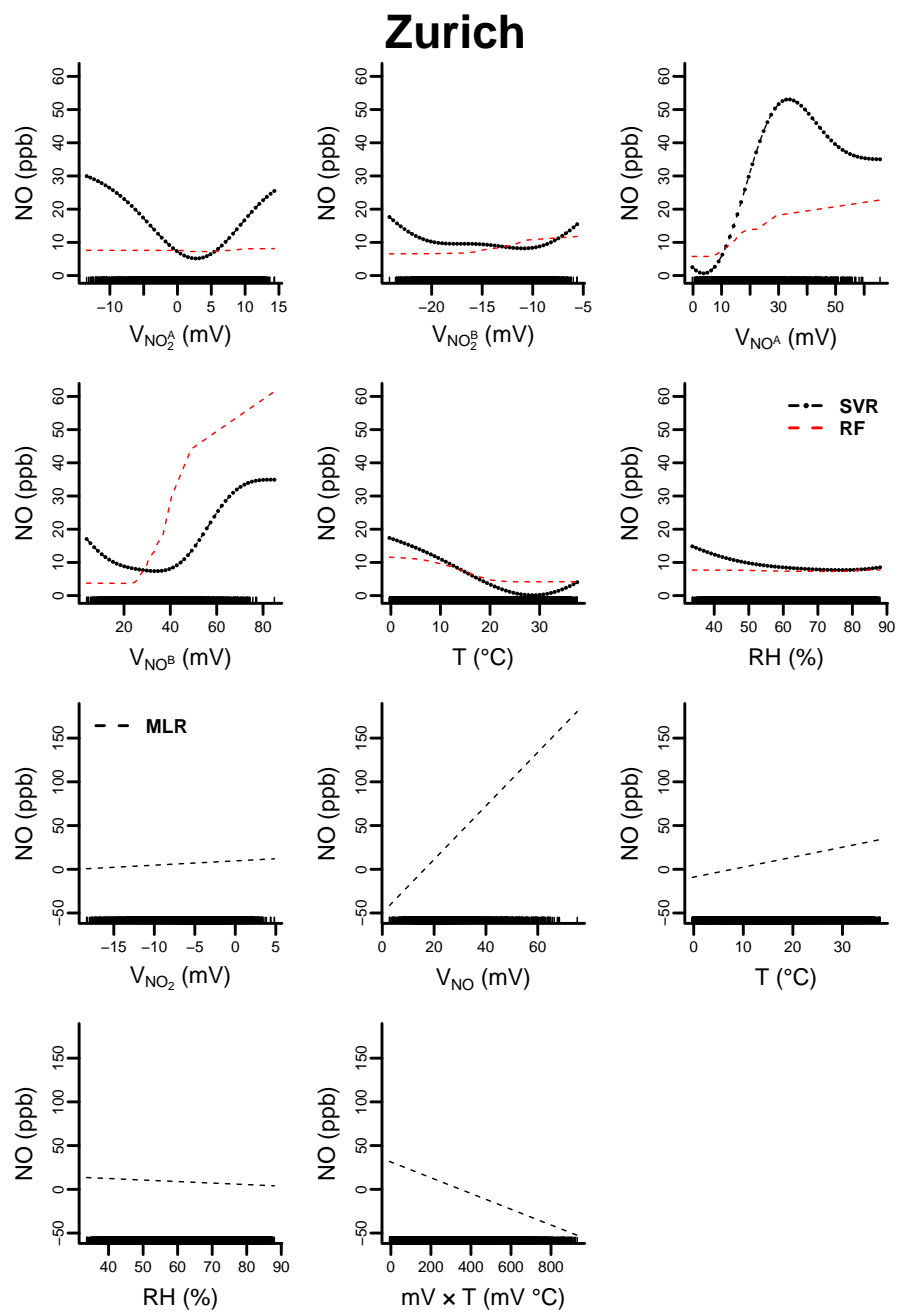


Figure S13: Partial plots for SVM, RF and MLR for the deployment dataset from SU009, NO. Rug on the abscissa indicates the range of the covariate.

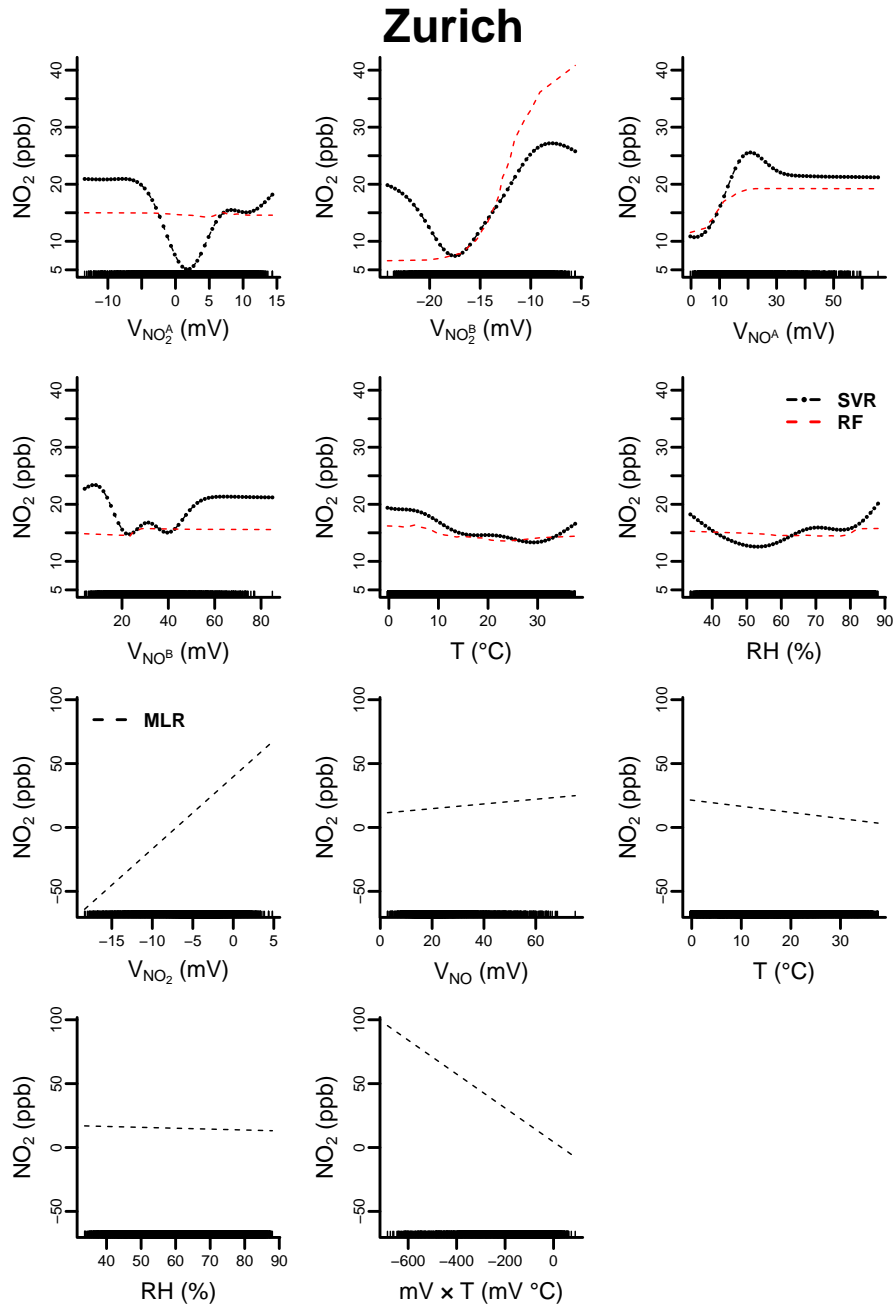


Figure S14: Partial plots for SVM, RF and MLR for the deployment dataset from SU009, NO_2 . Rug on the abscissa indicates the range of the covariate.

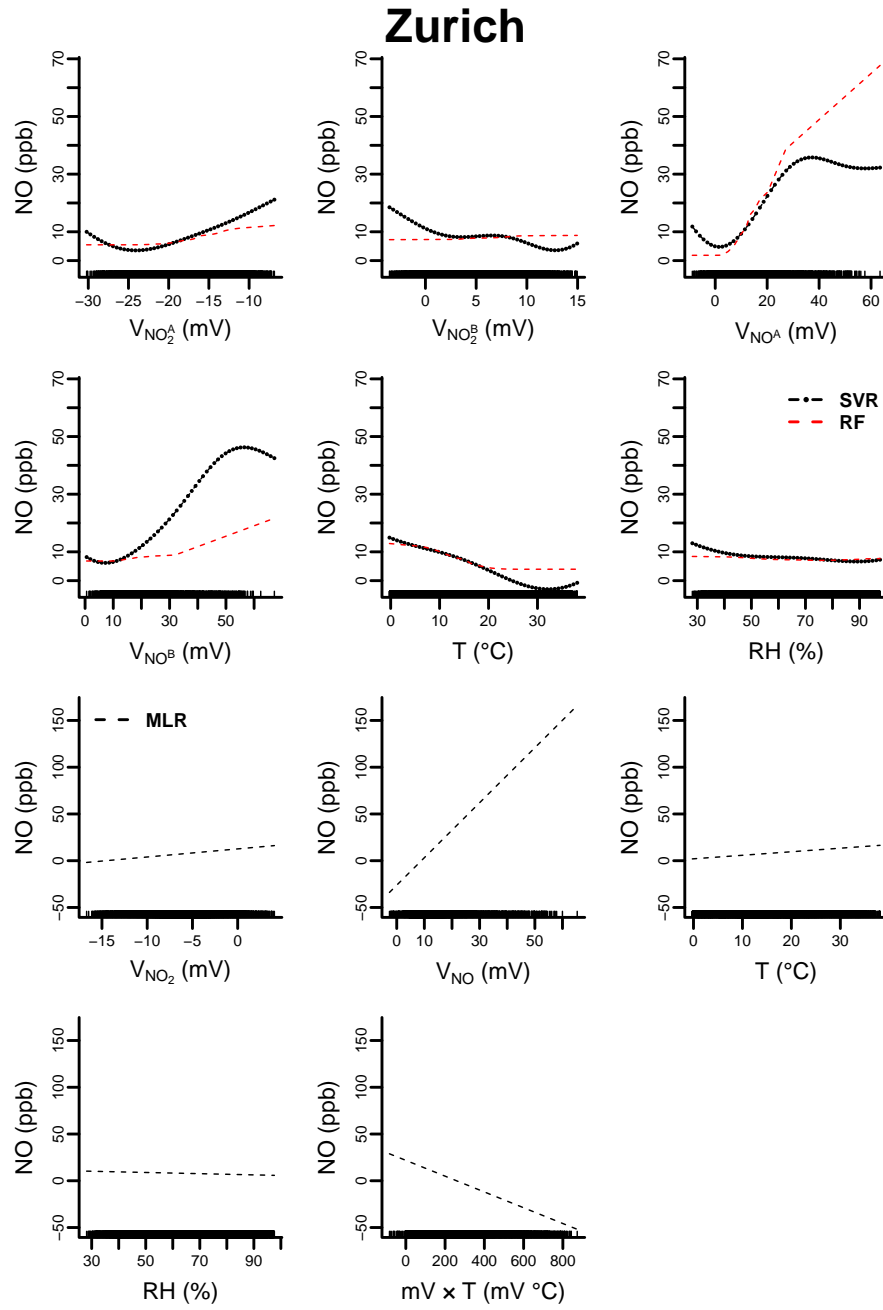


Figure S15: Partial plots for SVM, RF and MLR for the deployment dataset from SU010, NO. Rug on the abscissa indicates the range of the covariate.

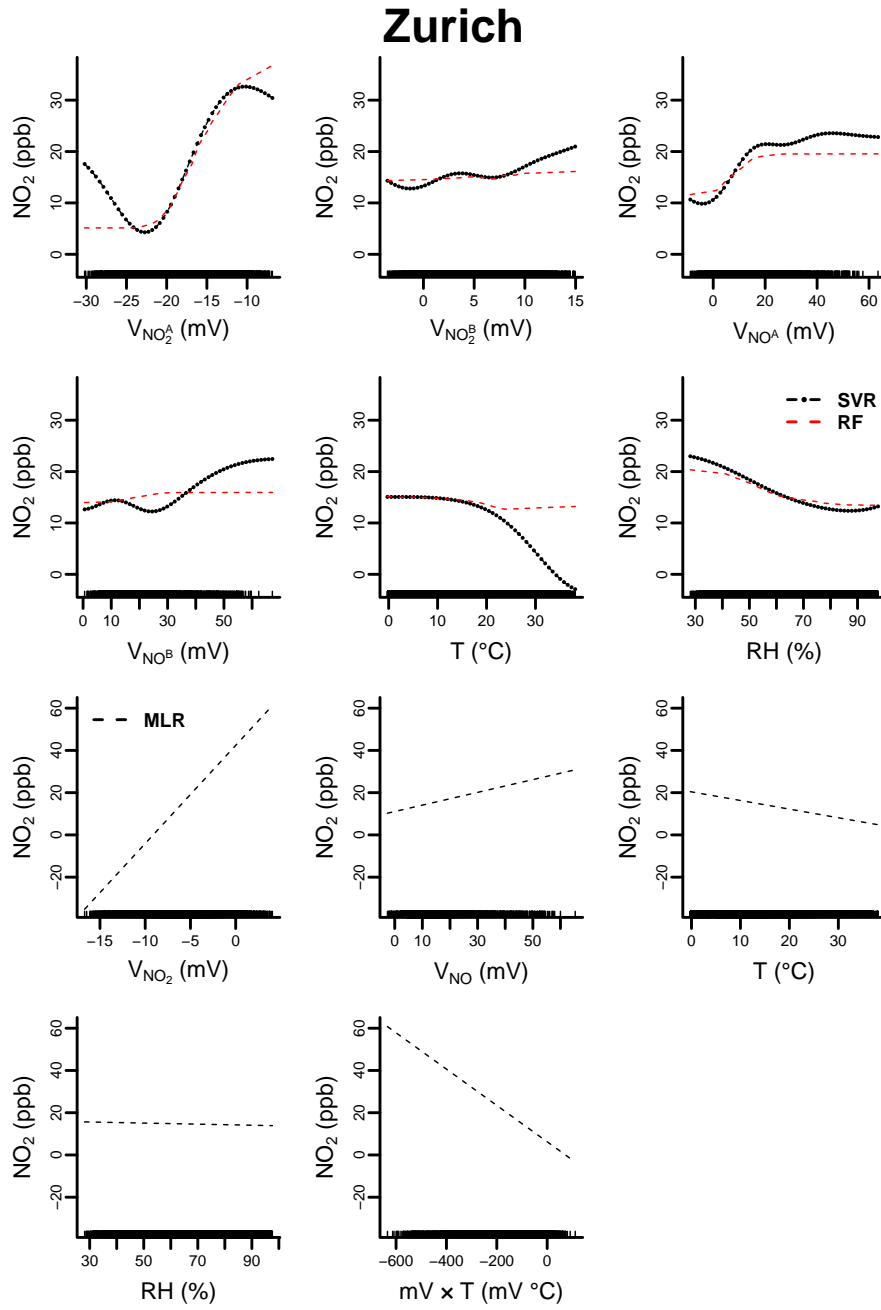


Figure S16: Partial plots for SVM, RF and MLR for the deployment dataset from SU010, NO_2 . Rug on the abscissa indicates the range of the covariate.

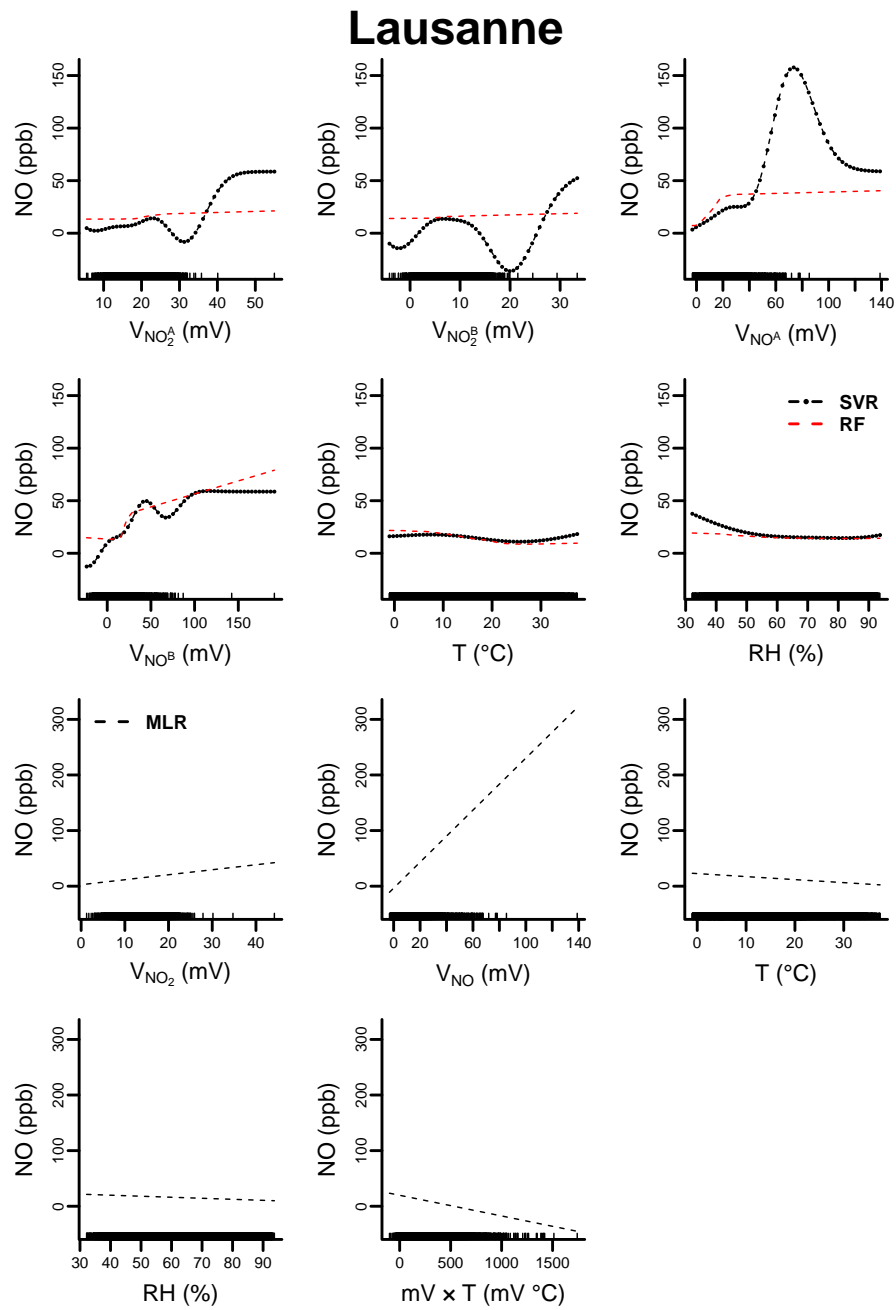


Figure S17: Partial plots for SVM, RF and MLR for the deployment dataset from SU011, NO. Rug on the abscissa indicates the range of the covariate.

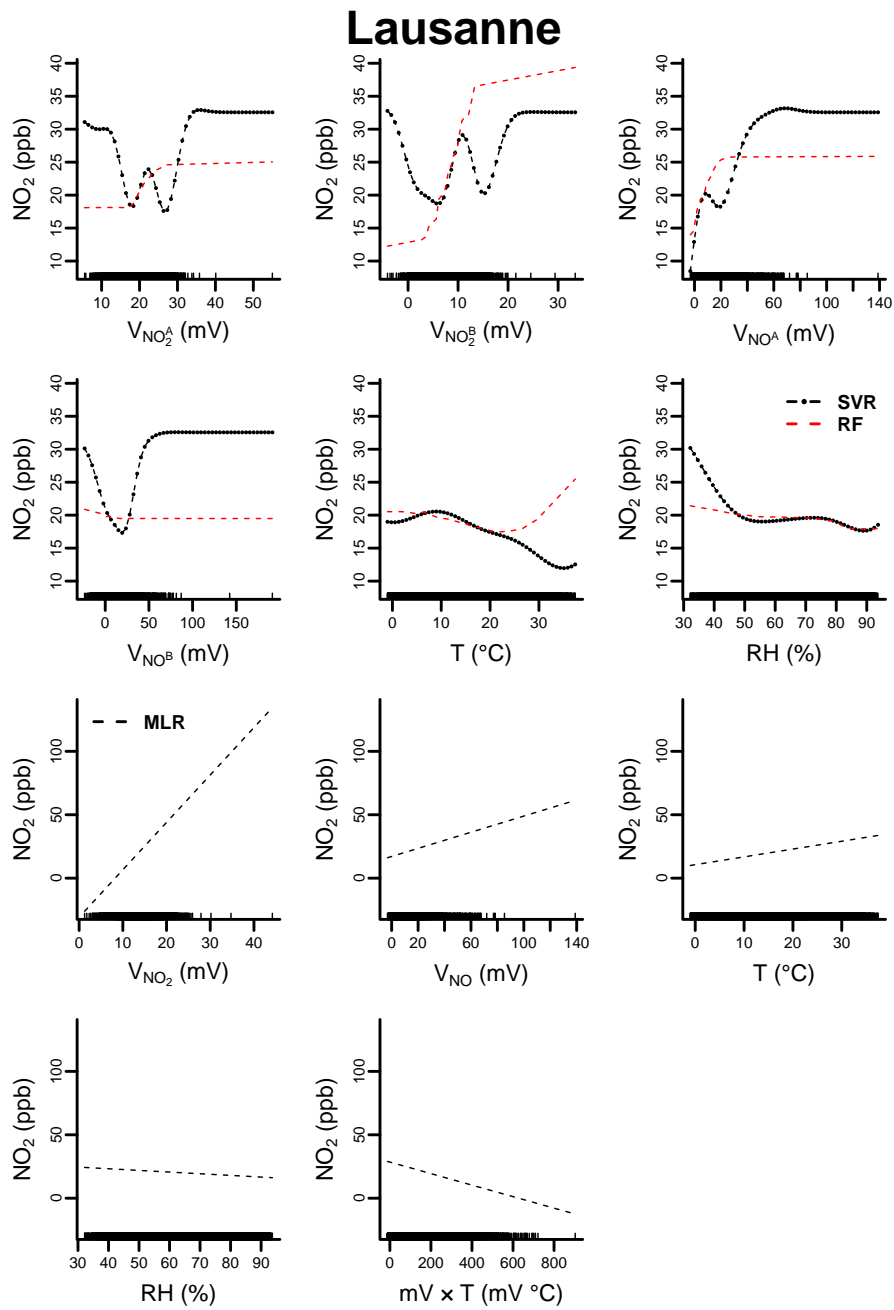


Figure S18: Partial plots for SVM, RF and MLR for the deployment dataset from SU011, NO_2 . Rug on the abscissa indicates the range of the covariate.

Lausanne

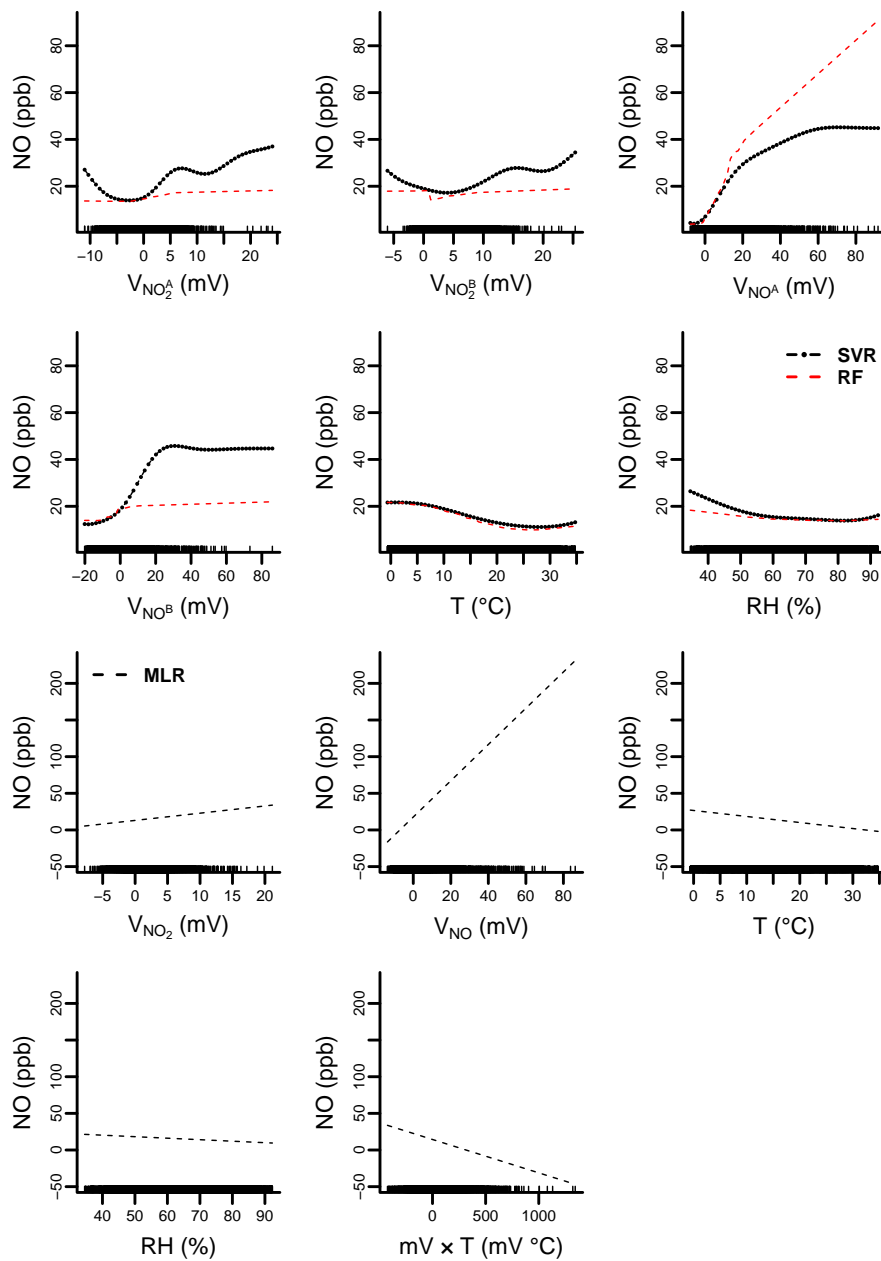


Figure S19: Partial plots for SVM, RF and MLR for the deployment dataset from SU012, NO. Rug on the abscissa indicates the range of the covariate.

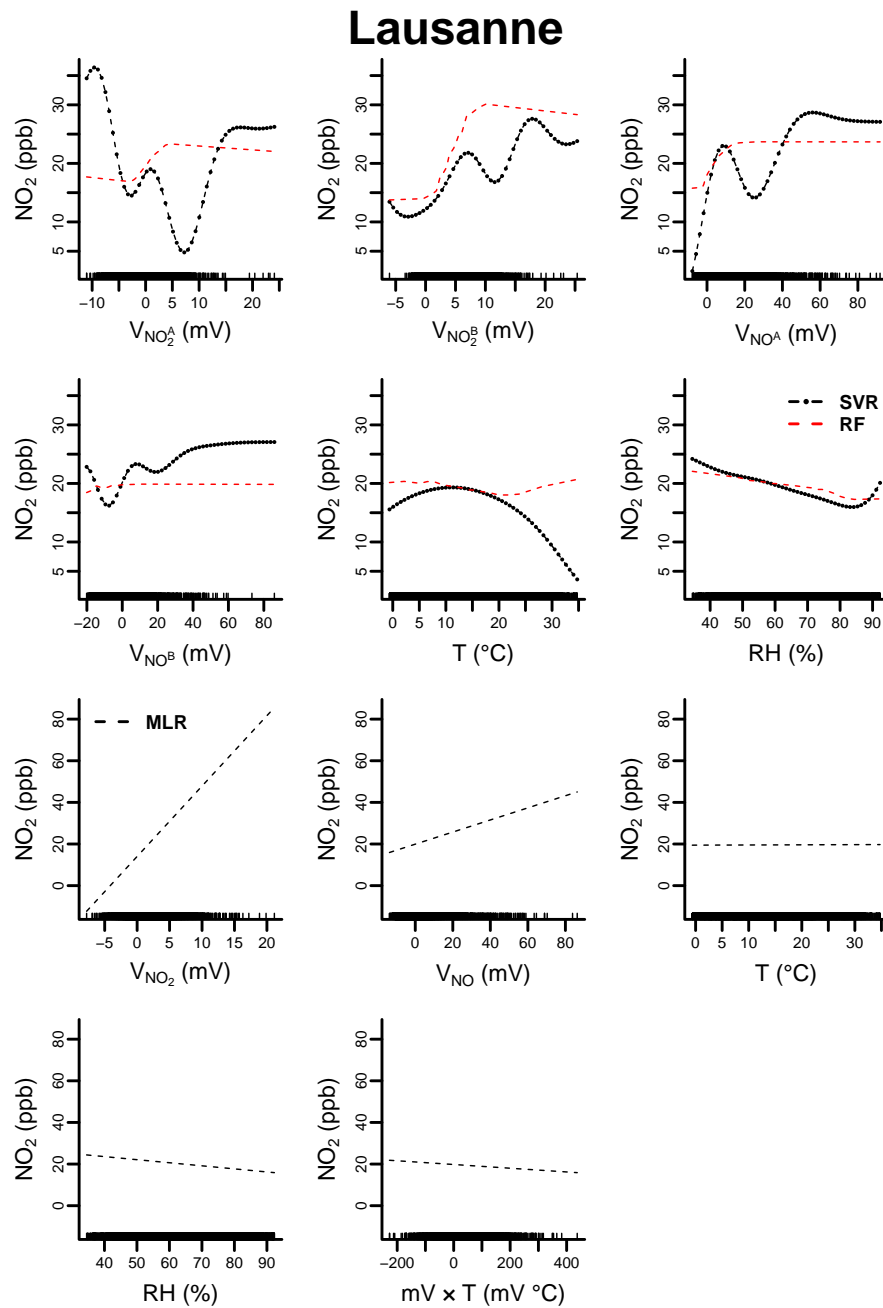


Figure S20: Partial plots for SVM, RF and MLR for the deployment dataset from SU012, NO_2 . Rug on the abscissa indicates the range of the covariate.

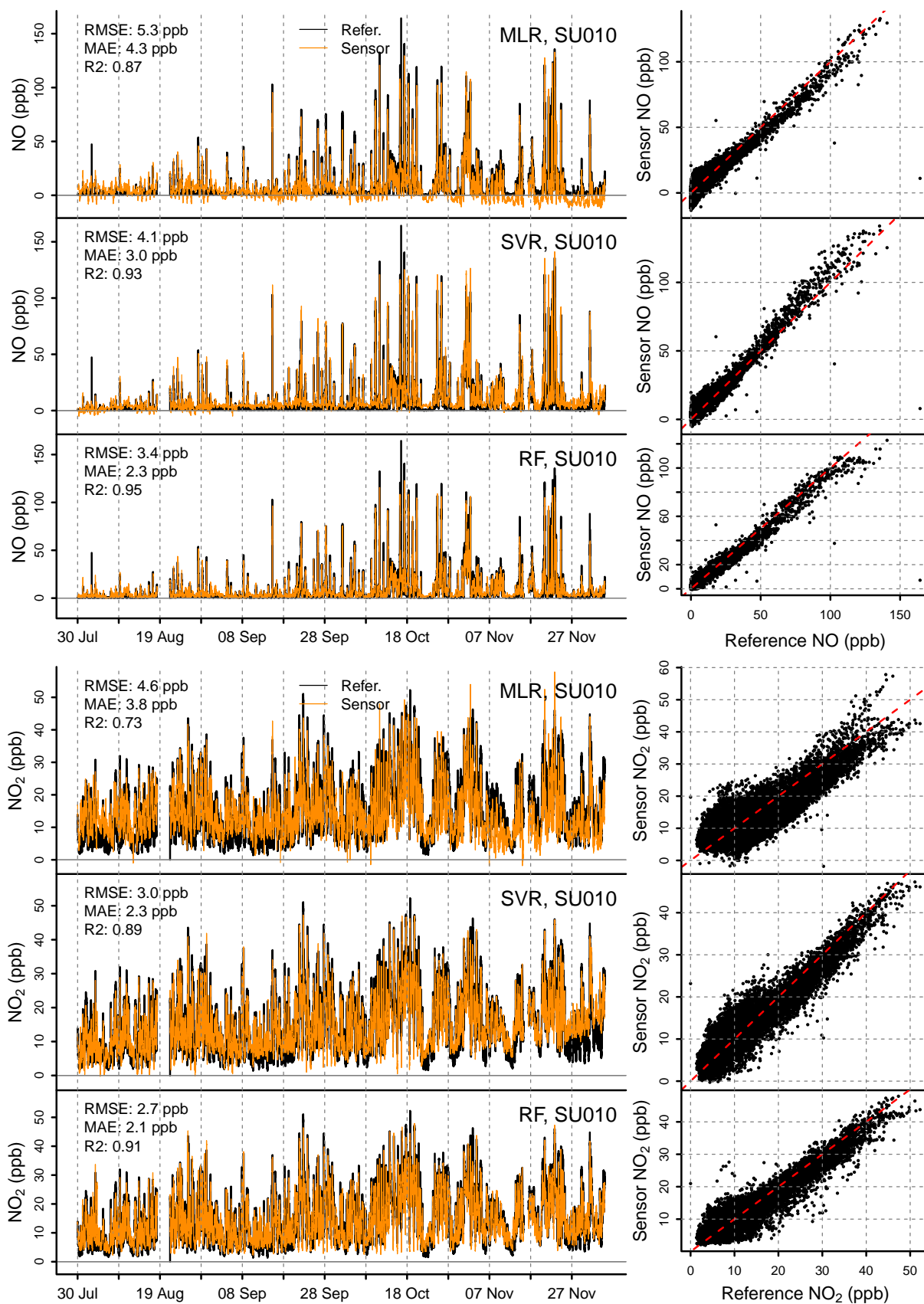


Figure S21: Comparison of NO (top) and NO₂ (bottom) estimates by SU010 with observations by reference instruments. 1:1 red dashed line is added in the scatterplots.

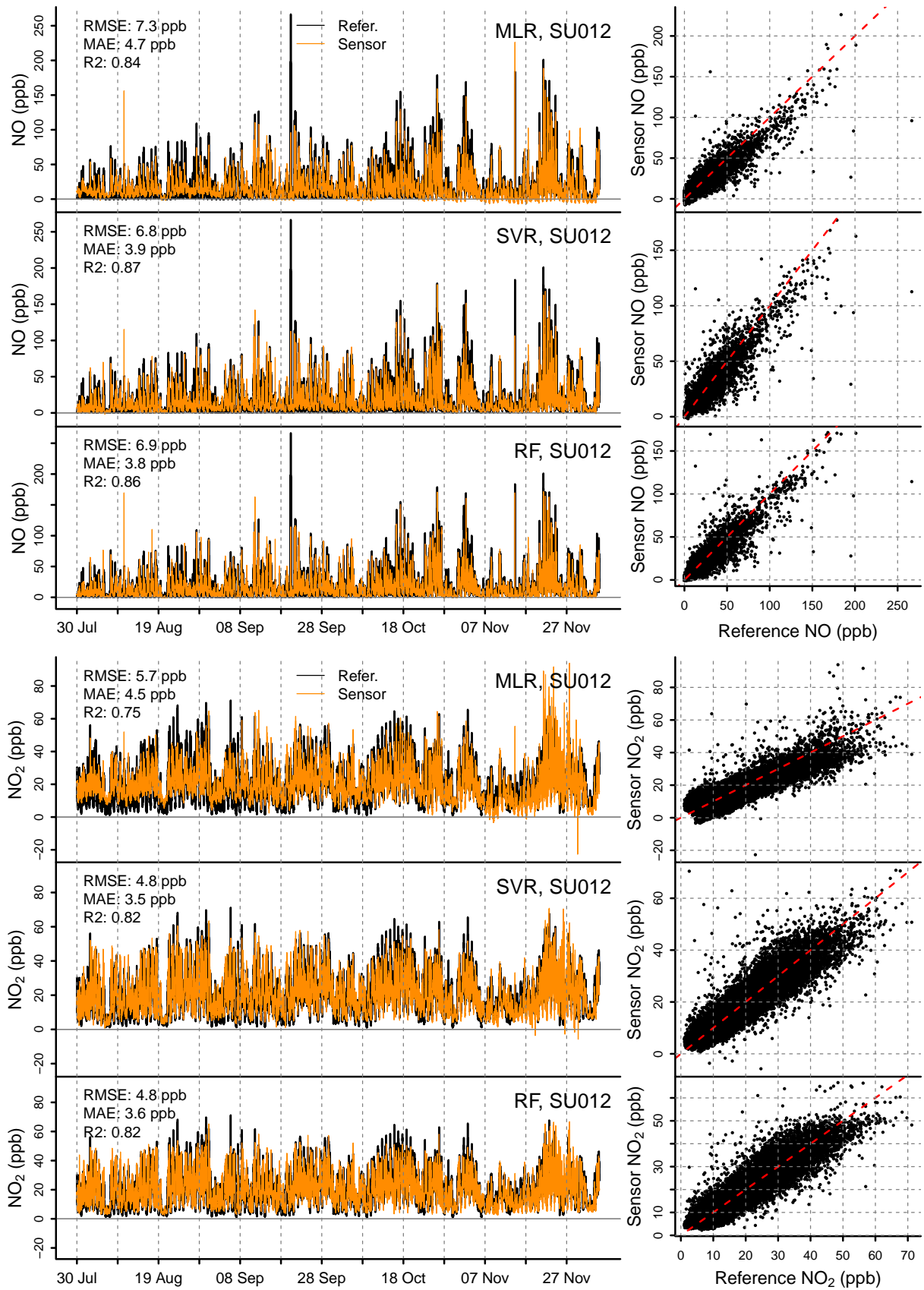


Figure S22: Comparison of NO (top) and NO₂ (bottom) estimates by SU012 with observations by reference instruments. 1:1 red dashed line is added in the scatterplots.

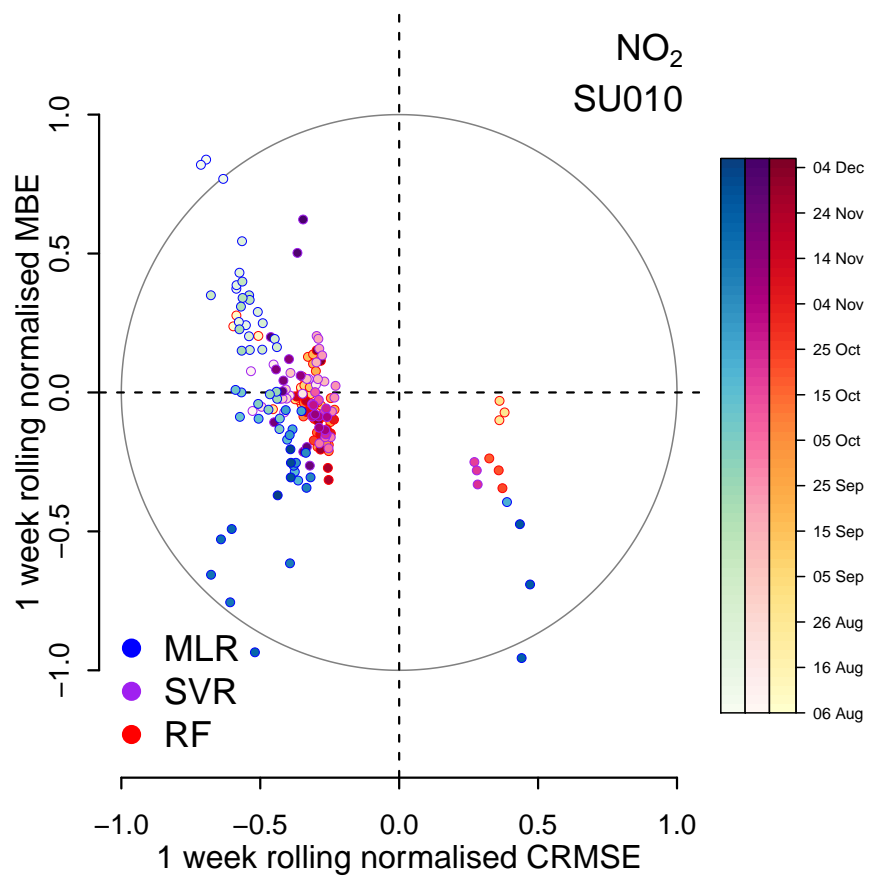
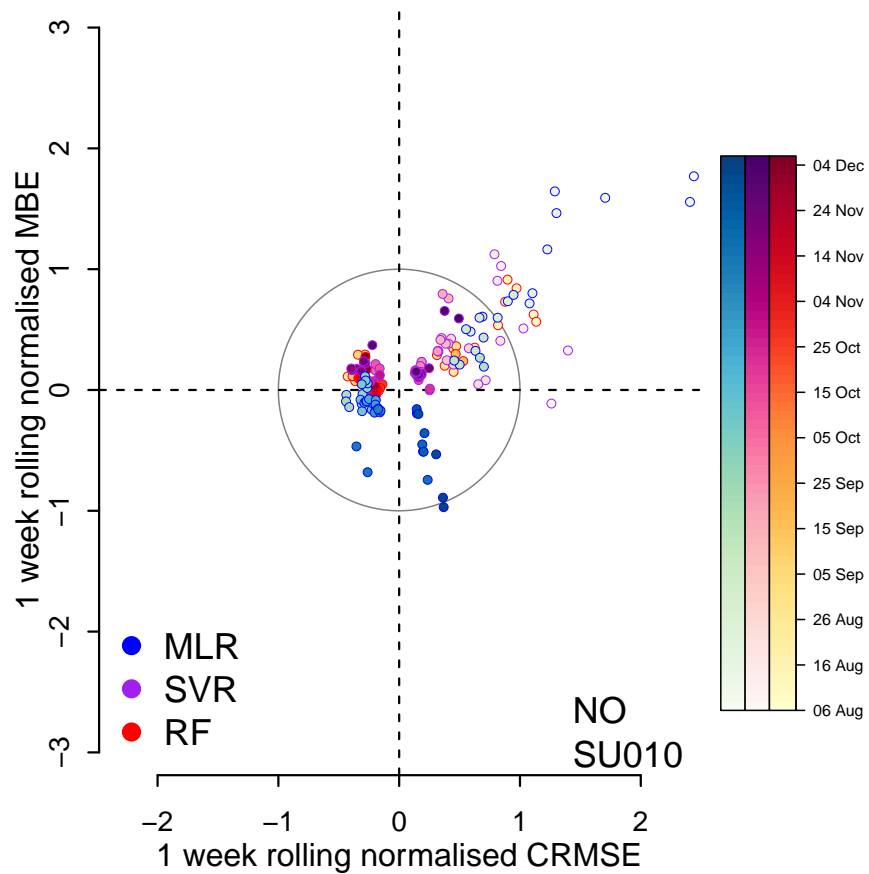


Figure S23: Target plot for the NO (top) and NO₂ (bottom) estimate by SU010.

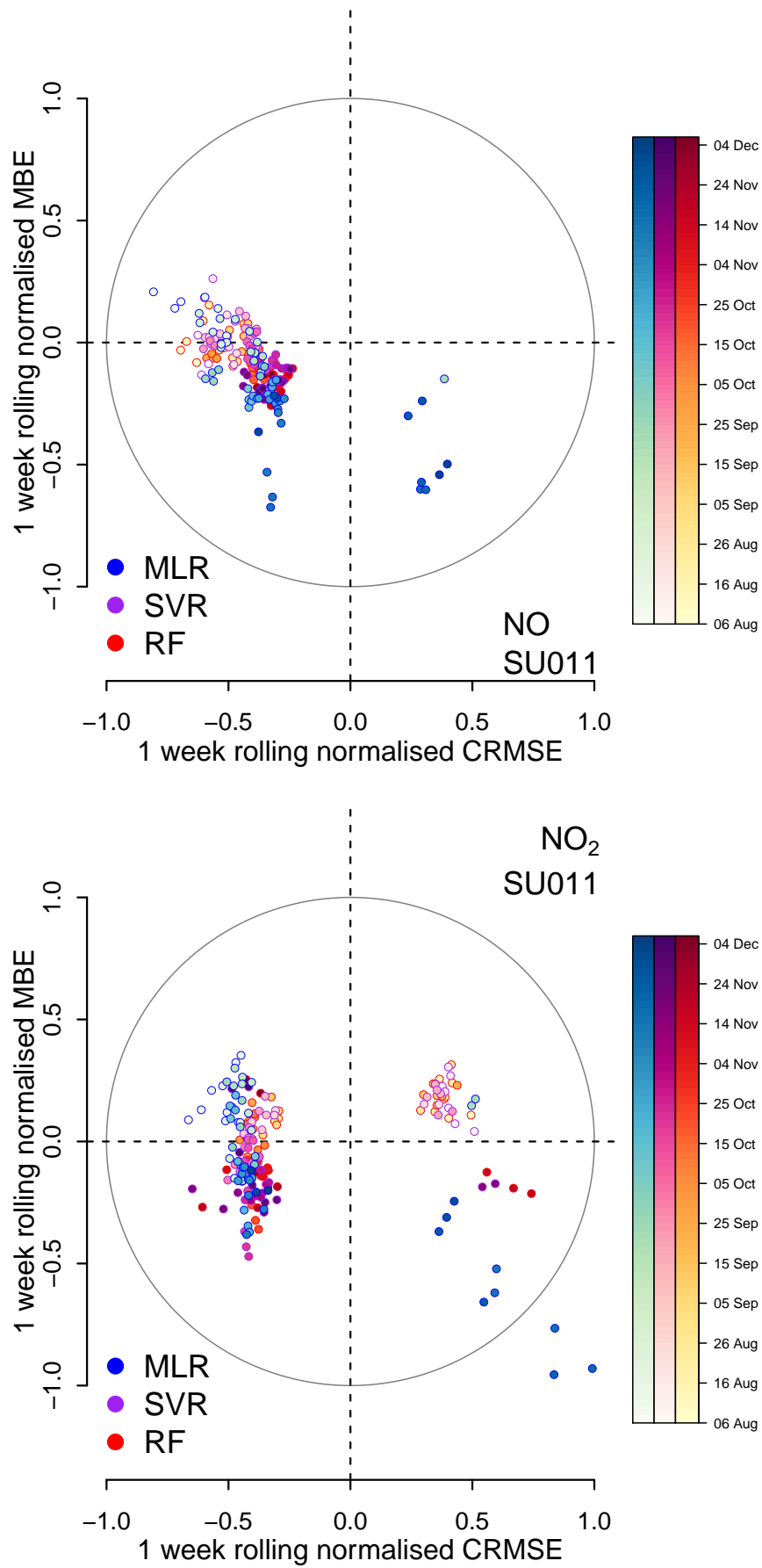


Figure S24: Target plot for the NO (top) and NO₂ (bottom) estimate by SU011.

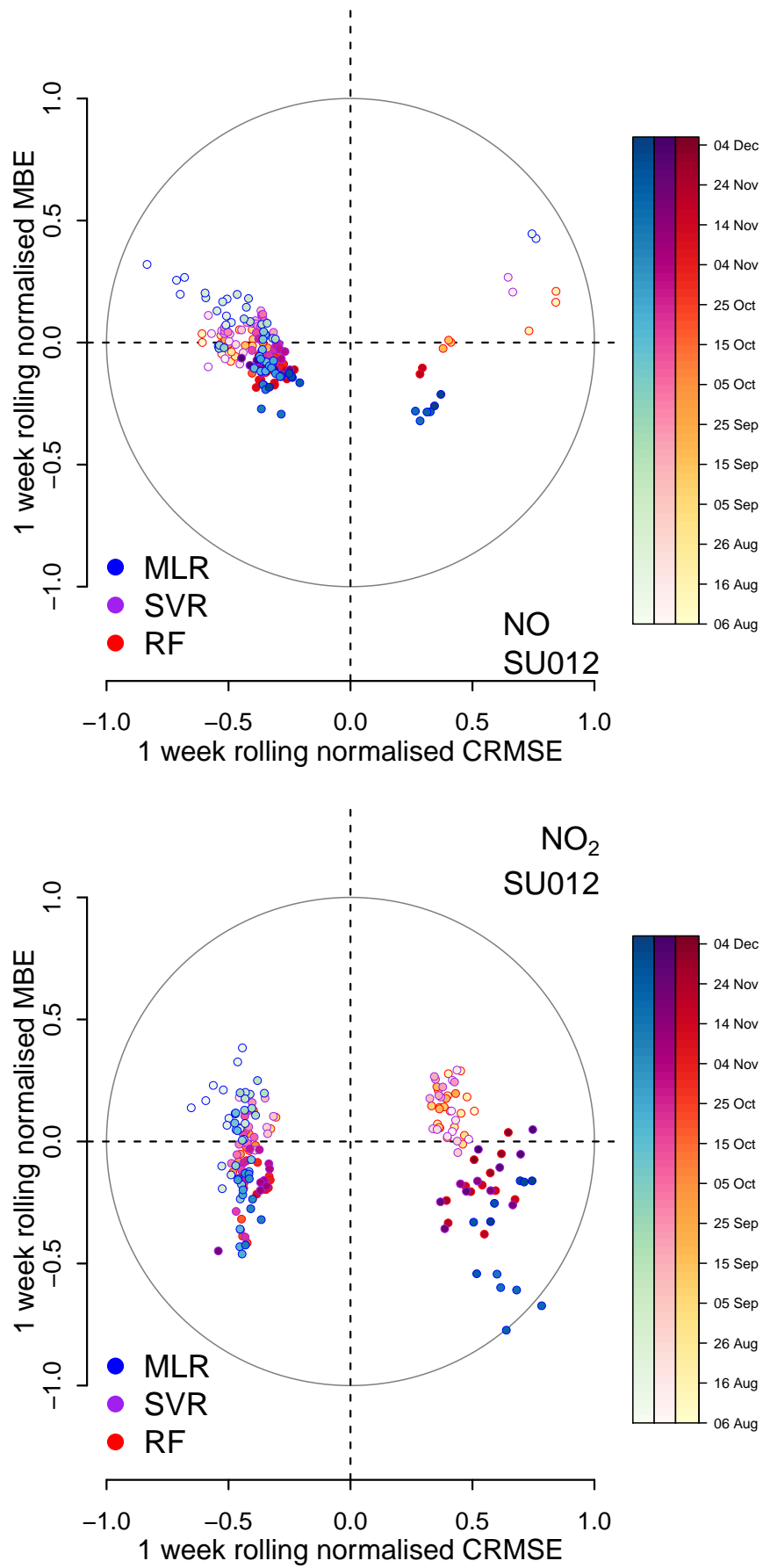


Figure S25: Target plot for the NO (top) and NO₂ (bottom) estimate by SU012.

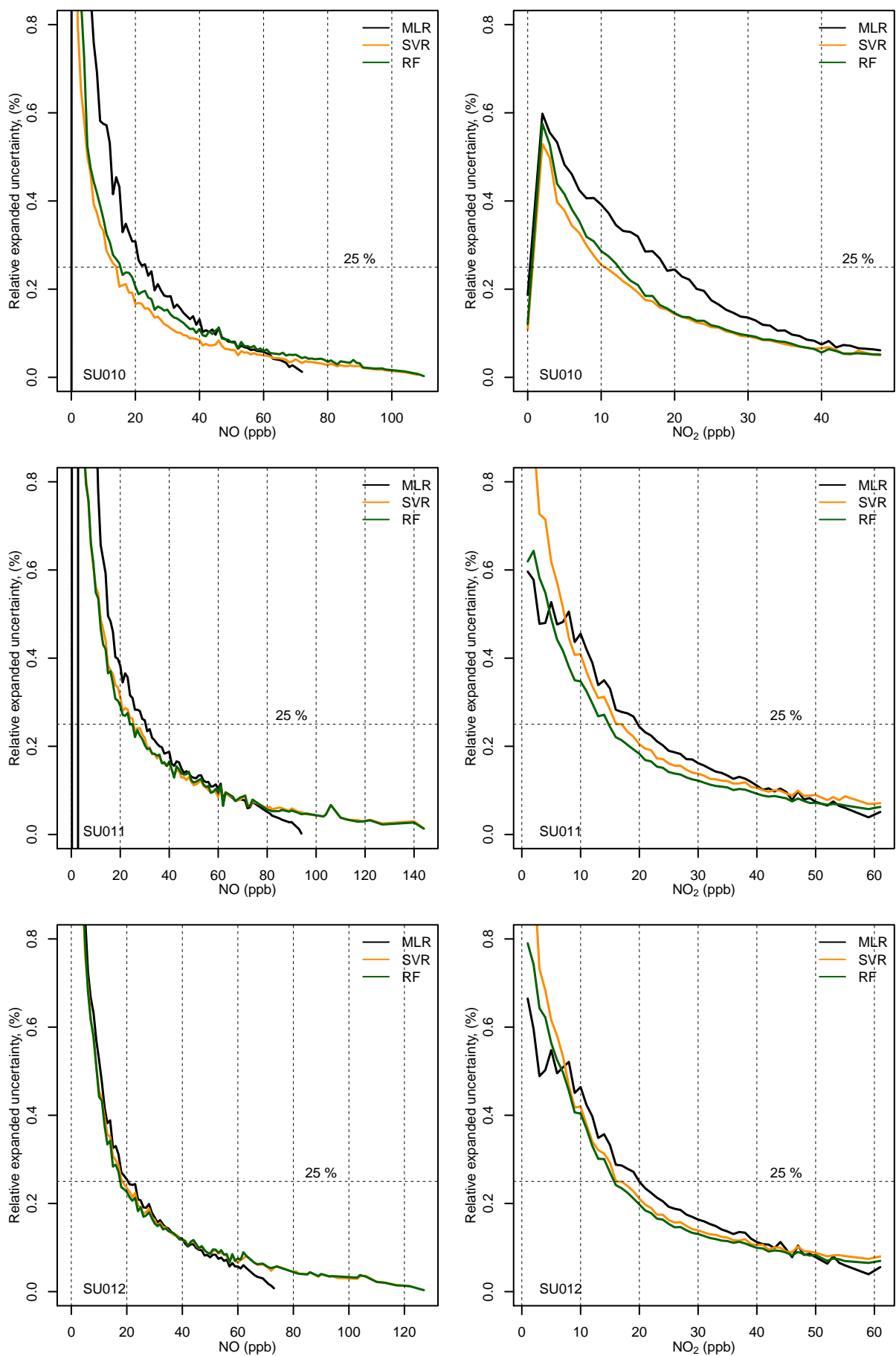


Figure S26: Comparison of expanded relative uncertainty and reference NO and NO₂ concentration for the SU010, SU011 and SU012, using 1 hour average data.

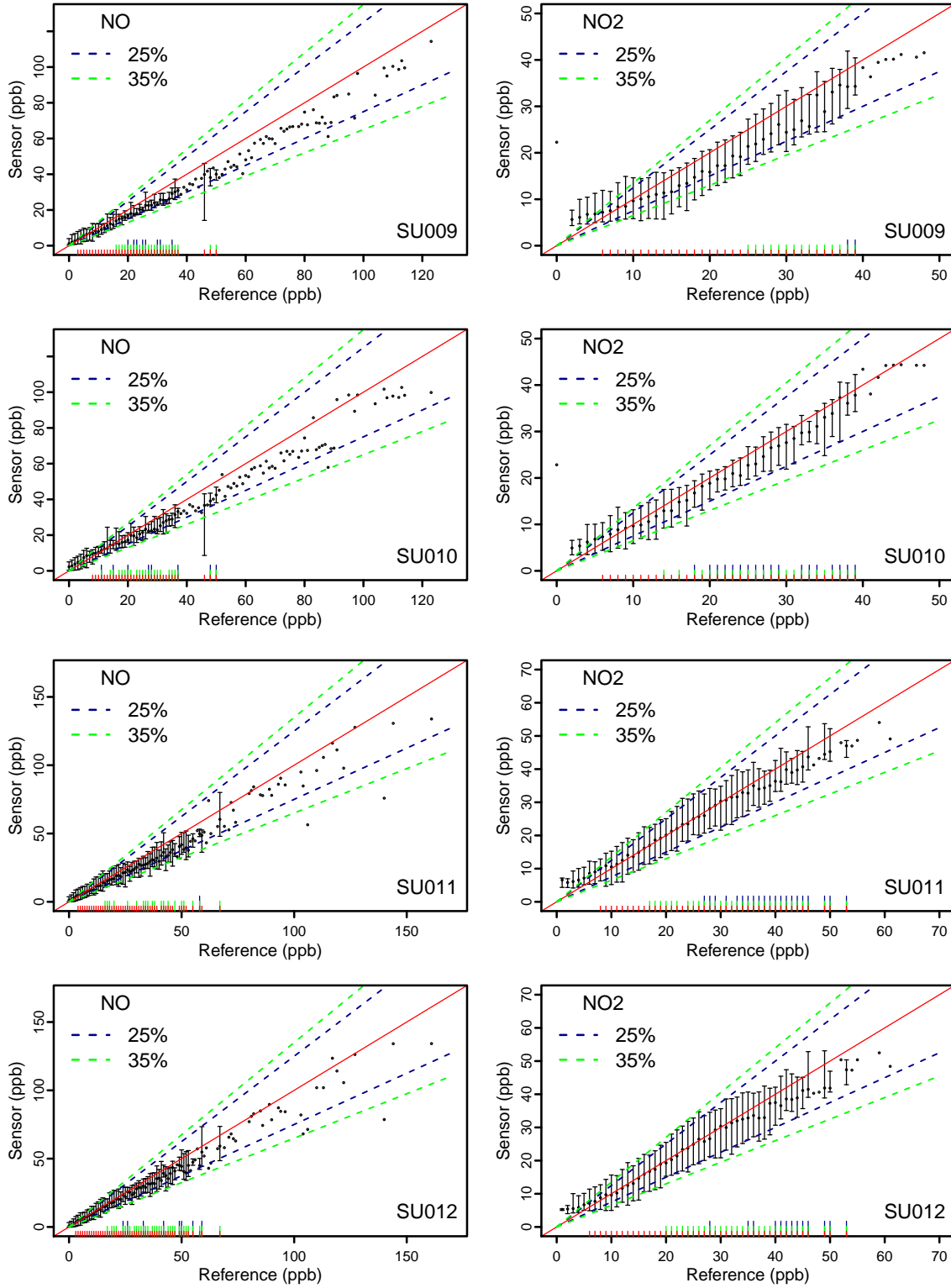


Figure S27: Range of the output using RF algorithm at the deployment sites. The reference data were binned by 1 ppb concentration interval. For each bin the median of the concentration estimated by the sensing device. When at least 10 readings were available, the 5th and 95th quantiles were included. 1:1 dashed line is added, along with its 25% and 35% uncertainty bands. Bottom red rug indicates if the median of sensor estimate is included in the in the 25% uncertainty bounds. Bottom green (blue) rug indicates if the 5–95% percentile range of estimates is included in the 35% (25%) uncertainty range.

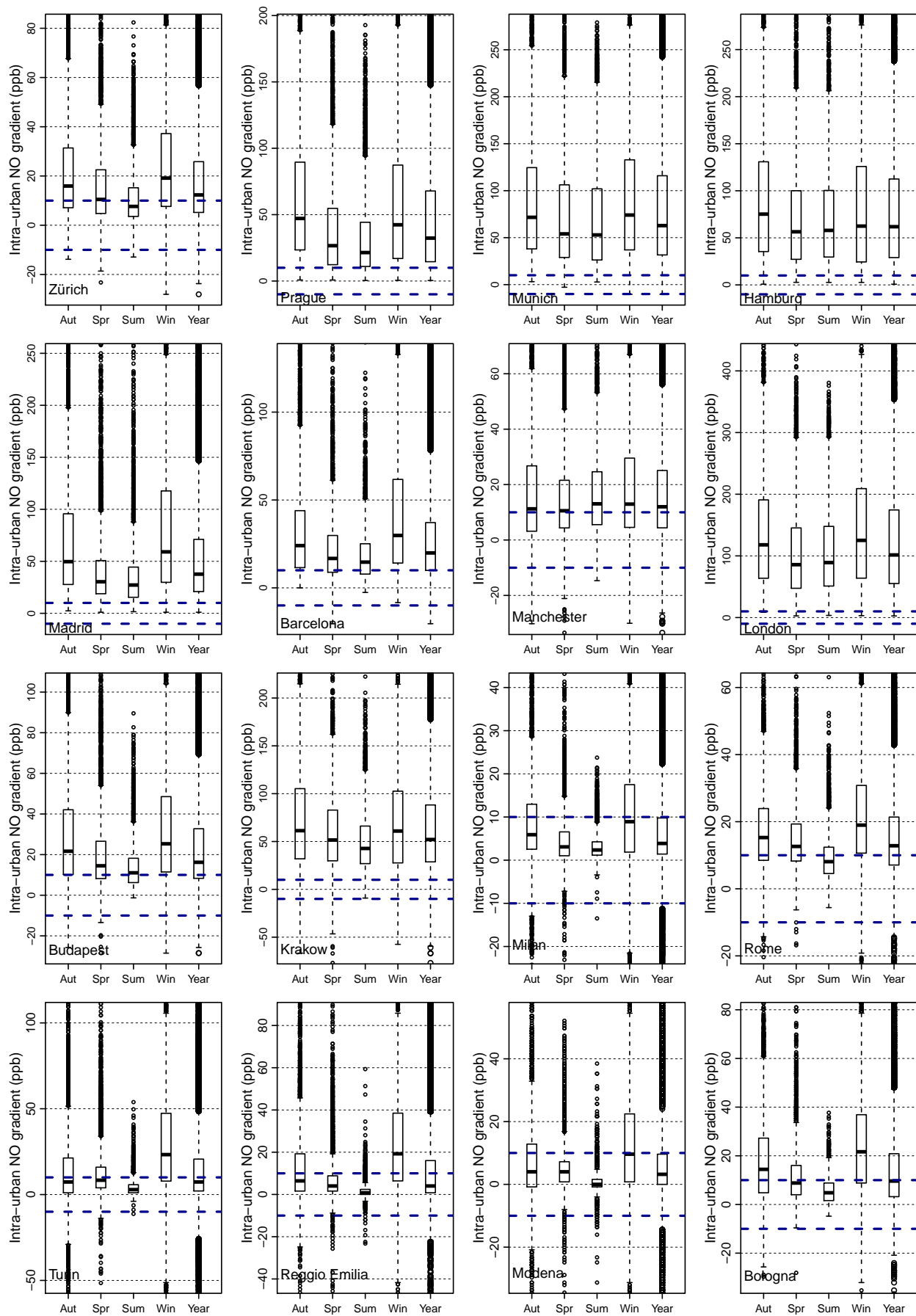


Figure S28: Seasonal boxplots of intra-urban NO gradient in a pool of European cities, proceeding from the station pairs having the largest difference in NO, on a hourly basis. Blue dashed lines indicate ± 10 ppb.

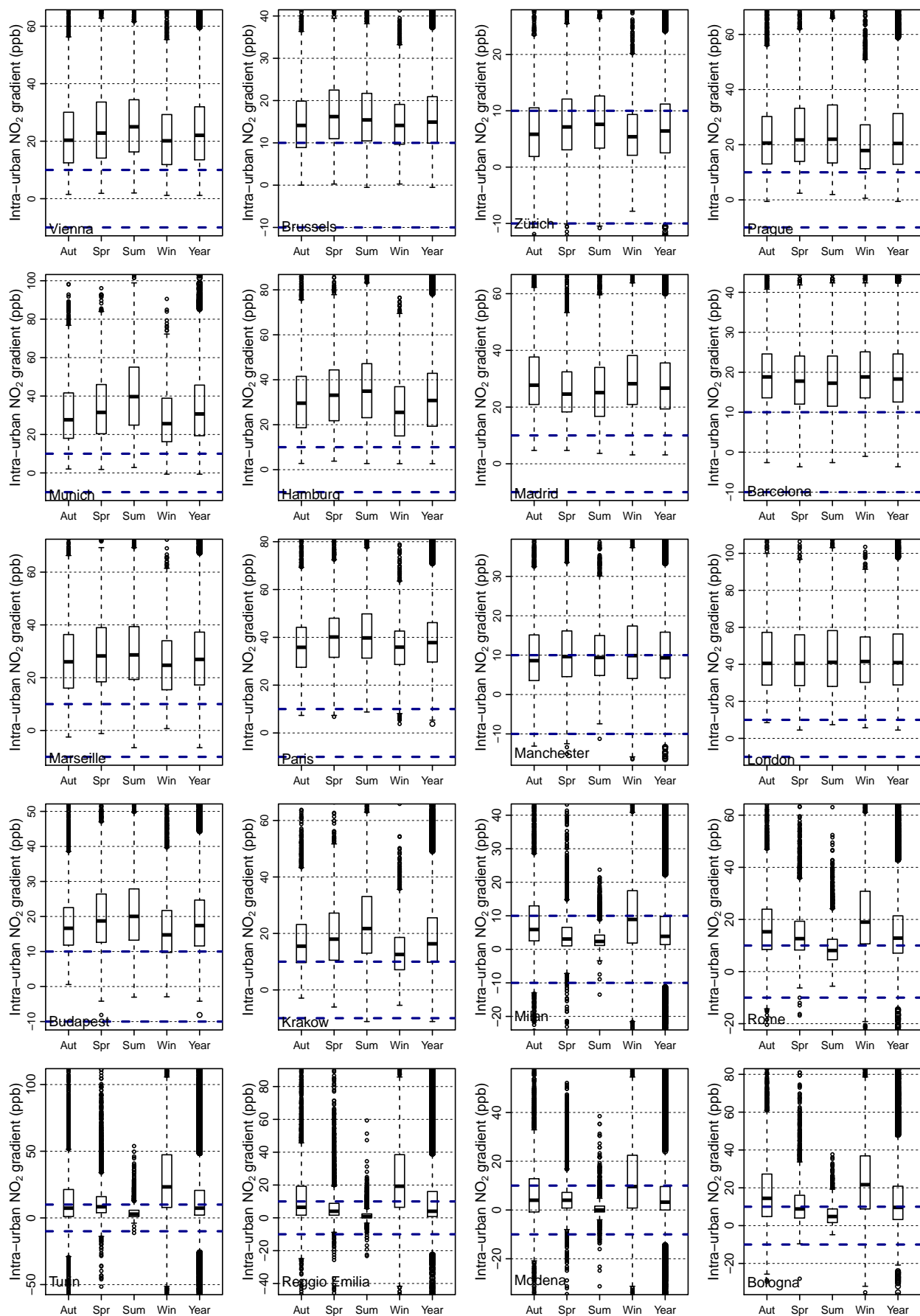


Figure S29: Seasonal boxplots of intra-urban NO_2 gradient in a pool of European cities, proceeding from the station pairs having the largest difference in NO_2 , on a hourly basis. Blue dashed lines indicate ± 10 ppb.

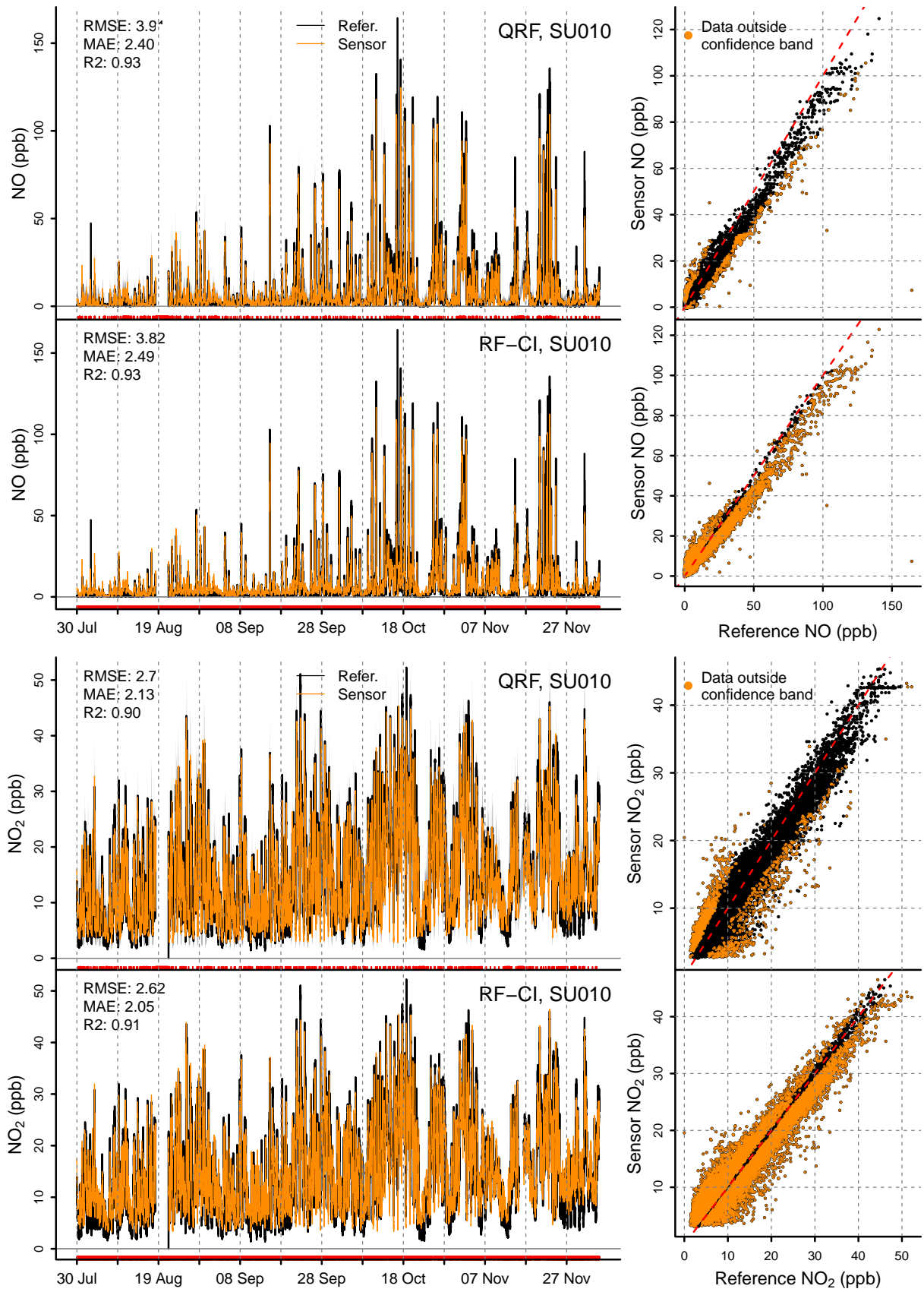


Figure S30: Comparison of QRF and CI-RF estimates of NO (top) and NO₂ (bottom) by SU010 with observations by reference instruments. 1:1 red dashed line is added in the scatterplots.

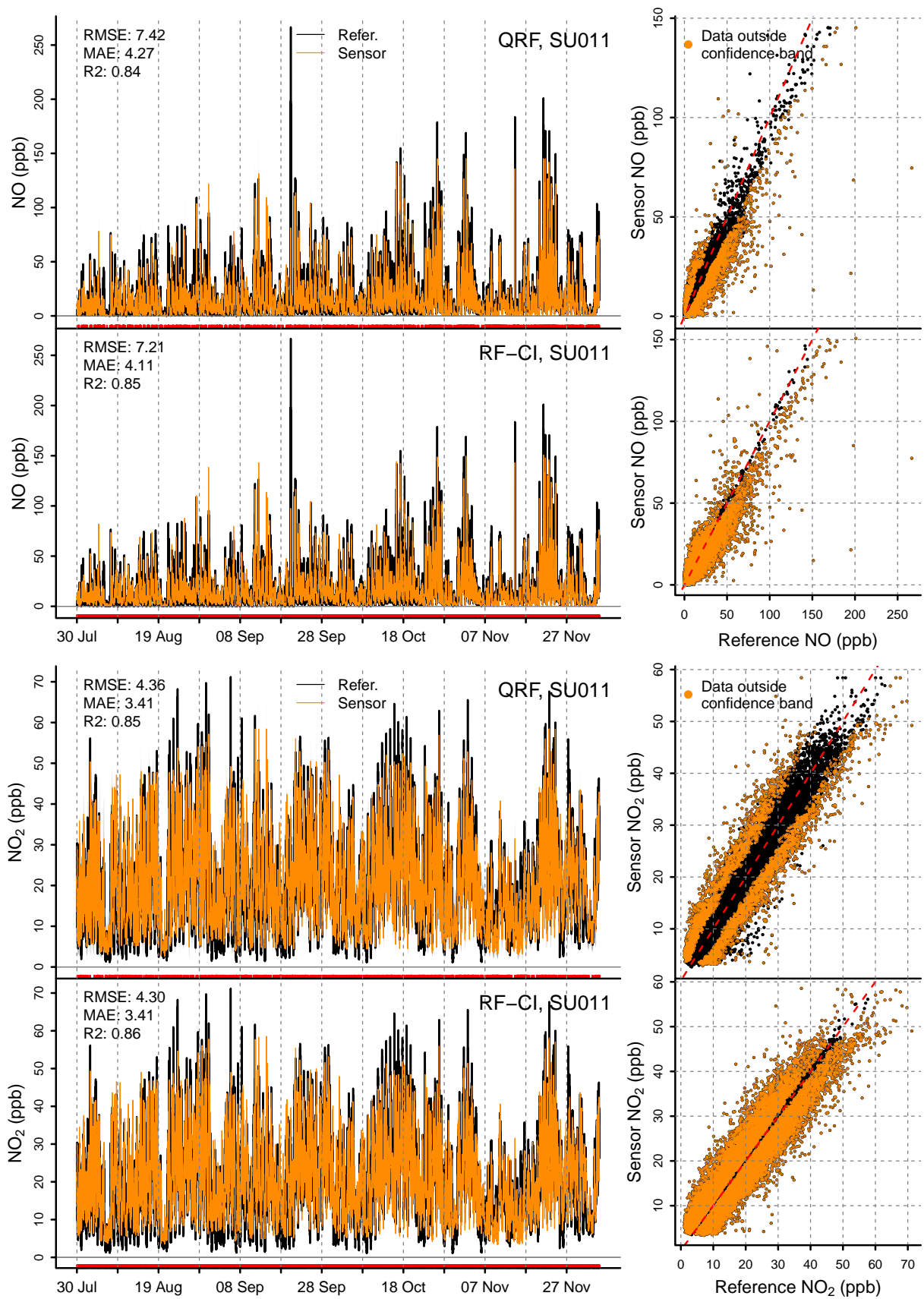


Figure S31: Comparison of QRF and CI-RF estimates of NO (top) and NO₂ (bottom) by SU011 with observations by reference instruments. 1:1 red dashed line is added in the scatterplots.

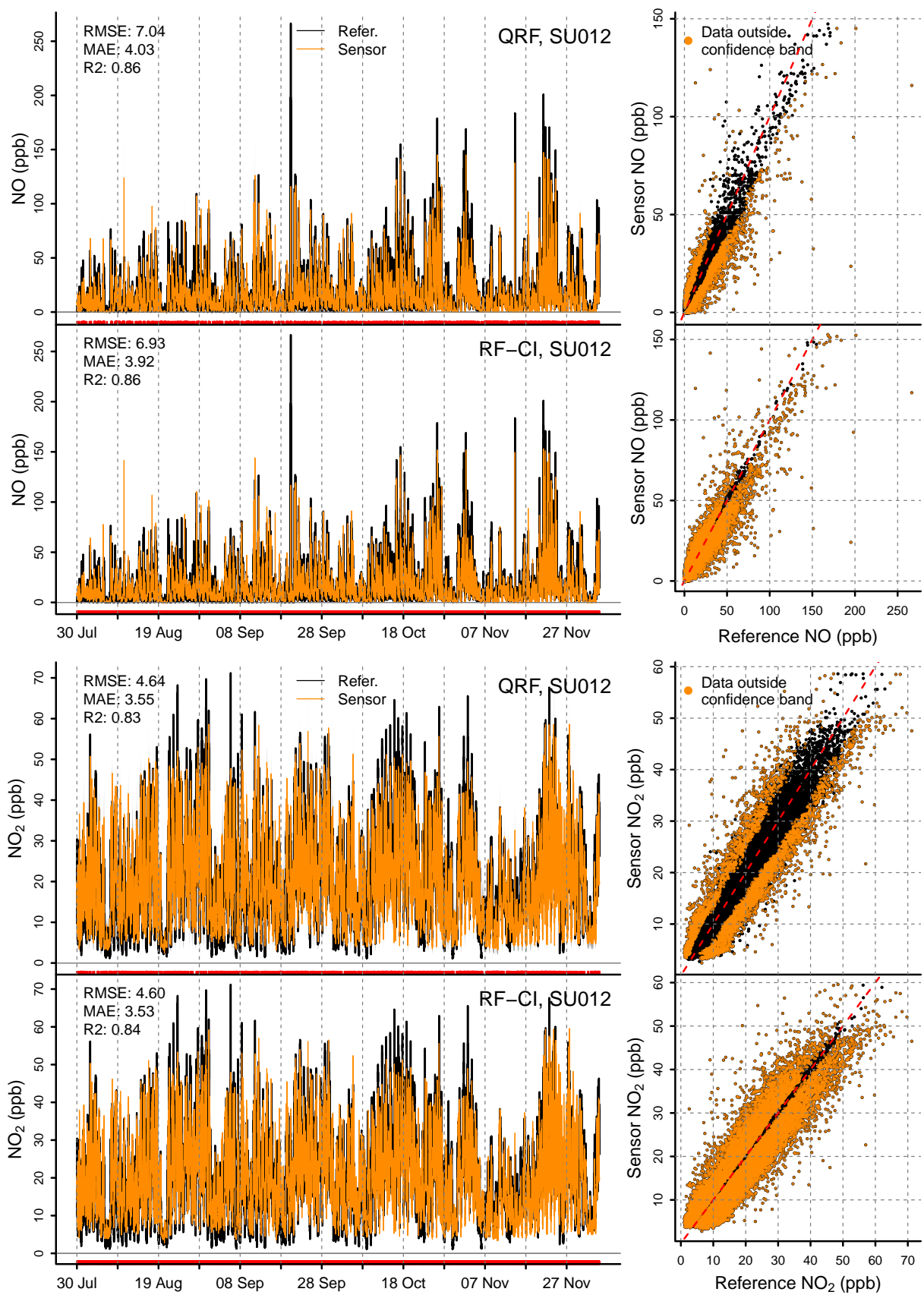


Figure S32: Comparison of QRF and CI-RF estimates of NO (top) and NO₂ (bottom) by SU012 with observations by reference instruments. 1:1 red dashed line is added in the scatterplots.